

Supporting Information

Mesoionic Carbene-based Self-Assembled Monolayers on Gold

Dianne S. Lee,^{a,b} Ishwar Singh,^{a,b} Alex J. Veinot,^{b,c} Mark D. Aloisio,^{a,b} Justin T. Lomax,^{b,c} Paul J. Ragona,^{b,c} Cathleen M. Crudden^{*a,b}

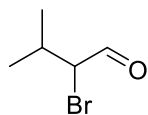
^a Department of Chemistry, Queen's University, 90 Bader Lane, Kingston, Ontario, Canada, K7L 3N6.

^b Carbon to Metal Coating Institute, C2MCI, Queen's University, 90 Bader Lane, Kingston, Ontario, Canada, K7L 4V1.

^c Department of Chemistry, Western University, London, Ontario N6A 3K7 and Surface Science Western, 999 Collip Cir, London, Ontario, Canada, N6G 0J3.

Syntheses

2-bromo-3-methylbutanal (4)



2-bromo-3-methylbutanal (**4**) was prepared following a modified literature procedure and used without isolation.⁵ A 500 mL round bottom flask was equipped with a PTFE-coated stir bar and 150 mL of CH₂Cl₂. Using an ice-water bath, the solvent was cooled to 0 °C before adding N-bromosuccinimide (17.8 g, 100 mmol, 1.3 eq) and L-proline (2.61 g, 23 mmol, 0.3 eq.). The round bottom flask was sealed with a septum and placed under an argon atmosphere. The red-orange coloured mixture was left to stir at 0 °C for 5 minutes before adding isovaleraldehyde (8.3 mL, 75 mmol, 1 eq.) drop-wise to the reaction mixture. The reaction mixture was left to warm to room temperature and was stirred under an argon atmosphere for 2 h. During this time, the colour of the reaction changed from red-orange, to pale yellow, before finally returning to red-orange. The reaction mixture was then concentrated to ca. 75 mL by rotary evaporation before adding 150 mL of hexanes to precipitate succinimide, L-proline and other impurities. The precipitates were removed by filtration through a 2.5 cm silica gel plug, washing with hexanes (3 x 50 mL). The colourless filtrate was then concentrated by rotary evaporation while maintaining the bath temperature below 40 °C, to afford the desired product as a pale yellow coloured oil (7.06 g, 57 %).

¹H NMR (CDCl₃, 700 MHz): δ 9.43 (d, *J* = 3.8 Hz, 1H, HCO), 4.06 (dd, *J* = 6.6 Hz, *J* = 3.8 Hz, 1H, CHBr), 2.23 (oct, *J* = 6.6 Hz, 1H, CH(CH₃)₂), 1.09 (d, *J* = 6.6 Hz, 3H, CH₃), 1.07 ppm (d, *J* = 6.6 Hz, 3H, CH₃).

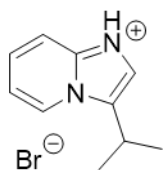
¹³C{¹H} NMR (CDCl₃, 175 MHz): δ 193.5, 63.8, 30.2, 20.4, 19.5 ppm.

Spectroscopic data were consistent with literature reports.⁶

General procedure for the preparation of 3-isopropylimidazo[1,2-a]pyridinium bromides

Crude 2-bromo-3-methylbutanal as prepared above was immediately dissolved in 50 mL anhydrous ethanol and combined with the desired 2-aminopyridine. A condenser was added, and the yellow-coloured solution was heated to 80 °C for 20 h while open to air. After cooling to room temperature, the volatiles were removed by rotary evaporation. The resulting pale yellow coloured solid was suspended in 100 mL of diethyl ether and triturated to afford a colourless precipitate and pale-yellow supernatant. The precipitate was isolated by vacuum filtration, washing with diethyl ether (3 x 25 mL) to afford the desired product as a pale yellow-coloured powder which was dried *in vacuo* overnight.

3-isopropylimidazo[1,2-a]pyridinium bromide (5•HBr)



Prepared following the general procedure above using 2-bromo-3-methylbutanal (6.3 g, 43 mmol, 1.2 eq.) and 2-aminopyridine (2.84 g, 30 mmol, 1 eq.). Product was obtained after drying *in vacuo* for 18 h (7.3 g, >99 %).

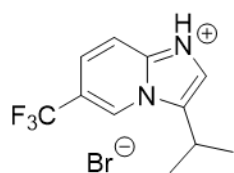
^1H NMR (CDCl_3 , 700 MHz): δ 15.1 (s, 1H, NH), 8.40 (s, br, 1H), 8.36 (d, $J = 9.3$ Hz, 1H), 7.81 (t, $J = 8.0$ Hz, 1H), 7.54 (d, $J = 2.7$ Hz, 1H, NCH), 7.46 (t, $J = 7.0$ Hz, 1H), 3.35 (sept, $J = 6.8$ Hz, 1H, CH), 1.44 ppm (d, $J = 6.8$ Hz, 6H, $\text{CH}-(\text{CH}_3)_2$).

$^{13}\text{C}\{^1\text{H}\}$ NMR (CDCl_3 , 175 MHz): δ 139.8, 132.8, 132.2, 125.1, 117.5, 117.4, 114.3, 24.0, 20.5 ppm.

Anal. calc. for $\text{C}_{10}\text{H}_{13}\text{N}_2\text{Br}$: C, 49.81; H, 5.43; N, 11.62. Found: C, 49.60; H, 5.38; N, 11.57.

ESI-HRMS (m/z): Calc. for $\text{C}_{10}\text{H}_{13}\text{N}_2^+$: 161.1074; found 161.1069.

3-isopropyl-6-trifluoromethylimidazo[1,2-a]pyridinium bromide



Prepared following the general procedure above using 2-bromo-3-methylbutanal (1.2 g, 7.4 mmol, 1.2 eq.) and 2-amino-5-trifluoromethylpyridine (1.0 g, 6.1 mmol, 1.0 eq.). Product was obtained after drying *in vacuo* for 18 h (1.1 g, 60 %).

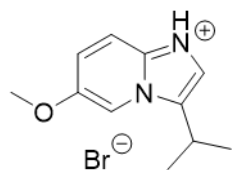
^1H NMR (600 MHz, CDCl_3) δ 8.69 (d, $J = 9.4$ Hz, 1H), 8.61 (p, $J = 1.1$ Hz, 1H), 7.98 (dd, $J = 9.4$, 1.6 Hz, 1H), 7.80 (d, $J = 1.0$ Hz, 1H), 3.46 – 3.37 (m, 1H, $\text{CH}-(\text{CH}_3)_2$), 1.53 (d, $J = 6.8$ Hz, 6H, $\text{CH}-(\text{CH}_3)_2$).

^{13}C NMR (151 MHz, CDCl_3) δ 140.15, 134.11, 127.81, 123.33, (q, $J = 35.7$ Hz, CF_3), 119.47, 115.92, 24.02, 20.53.

^{19}F NMR (470 MHz, CDCl_3) δ -62.31.

ESI-HRMS (m/z): Calc. for $\text{C}_{11}\text{H}_{12}\text{F}_3\text{N}_2^+$: 229.10; found 229.09.

3-isopropyl-6-methoxyimidazo[1,2-a]pyridinium bromide



Prepared following the general procedure above using 2-bromo-3-methylbutanal (2.3 g, 14 mmol, 1.2 eq.) 2-Amino-5-methoxypyridine (1.5 g, 12 mmol, 1.0 eq.). The product was obtained after drying *in vacuo* for 18 h (2.9 g, 90 %).

^1H NMR (500 MHz, CDCl_3) δ 14.50 (s, 1H, NH), 8.09 (d, $J = 7.5$ Hz, 1H), 7.63 (d, $J = 2.5$ Hz, 1H), 7.30 (d, $J = 2.6$ Hz, 1H), 7.00 (dd, $J = 7.5$, 2.5 Hz, 1H), 3.99 (s, 3H, $\text{O}-\text{CH}_3$), 3.21 (hept, $J = 6.8$ Hz, 1H, $\text{CH}-(\text{CH}_3)_2$), 1.40 (d, $J = 6.8$ Hz, 6H, $\text{CH}-(\text{CH}_3)_2$).

^{13}C NMR (126 MHz, CDCl_3) δ 162.84, 142.49, 131.55, 125.42, 116.20, 112.08, 92.37, 57.17, 23.84, 20.67.

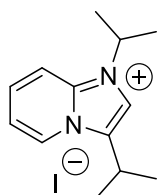
ESI-HRMS (m/z): Calc. for $\text{C}_{11}\text{H}_{15}\text{N}_2\text{O}^+$: 191.12; found 191.11774.

General procedure for the preparation of 1,3-diisopropylimidazol[1,2-a]pyridinium iodides

Pretreatment: A solution of desired 3-isopropylimidazo[1,2-*a*]pyridinium bromide in CHCl₃ (100 mL) was prepared and transferred to a separatory funnel. The yellow coloured organic solution was washed with a saturated aqueous NaHCO₃ solution (2 x 50 mL), followed by a saturated NaCl solution (50 mL). After separating the aqueous and organic portions and removing the CHCl₃ by rotary evaporation, 3-isopropylimidazo[1,2-*a*]pyridine was obtained as an orange coloured oil and used immediately without further isolation.

N-alkylation: 3-isopropylimidazo[1,2-*a*]pyridine derivatives, as prepared above, were dissolved in acetonitrile (100 mL) and combined with 2-iodopropane in a 250 mL round bottom flask. A PTFE-coated magnetic stir bar was added before fitting a water-cooled condenser and heating to 85 °C for 20 h while open to air. After cooling to room temperature, the volatiles were removed by rotary evaporation, yielding a yellow coloured residue which was suspended in an acetone/diethyl ether mixture (1:1, 40 mL). After sonication/trituration, the colourless precipitate was collected by vacuum filtration and washed with diethyl ether (3 x 20 mL) to afford the desired product as a pale yellow powder.

1,3-diisopropylimidazol[1,2-*a*]pyridinium iodide (MIC^{iPr}•HI)



Prepared following the general procedure above using 3-isopropylimidazo[1,2-*a*]pyridinium bromide (6.03 g, 25 mmol, 1 eq.), 2-iodopropane (7.5 mL, 75 mmol, 3.0 eq.). Product was obtained after drying *in vacuo* for 18 h (6.79 g, 82%).

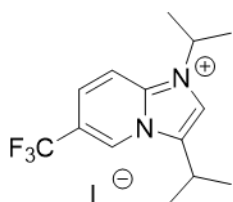
¹H NMR (CDCl₃, 500 MHz): δ 8.73 (d, *J* = 7.0 Hz, 1H), 8.42 (d, *J* = 9.1 Hz, 1H), 8.01 (t, *J* = 8.0 Hz, 1H), 7.82 (s, 1H), 7.60 (t, *J* = 7.0 Hz, 1H), 5.37 (sept, *J* = 6.7 Hz, 1H, CH-(CH₃)₂), 3.53 (sept, *J* = 6.8 Hz, 1H, CH-(CH₃)₂), 1.70 (d, *J* = 6.7 Hz, 6H, CH-(CH₃)₂), 1.49 ppm (d, *J* = 6.8 Hz, 6H, CH-(CH₃)₂).

¹³C{¹H} NMR (CDCl₃, 125 MHz): δ 138.4, 134.0, 133.6, 127.0, 118.2, 117.4, 112.7, 51.1, 24.4, 22.9, 20.8 ppm.

Anal. calc. for C₁₃H₁₉N₂I: C, 47.29; H, 5.80; N, 8.48. Found: C, 47.24 H, 5.77; N, 8.44.

ESI-HRMS (*m/z*): Calc. for C₁₃H₁₉N₂⁺: 203.1543; found 203.1534.

1,3-diisopropyl-6-trifluoromethylimidazol[1,2-*a*]pyridinium iodide



Prepared following the general procedure above using 3-isopropyl-6-trifluoromethylimidazo[1,2-*a*]pyridinium bromide (2 g, 6.4 mmol, 1 eq.), 2-iodopropane (5.3 mL, 27 mmol, 4.3 eq.). The product material was obtained after drying *in vacuo* for 18 h (1.2 g, 48%).

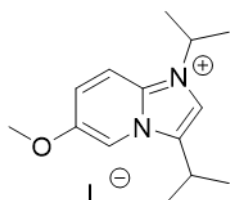
¹H NMR (600 MHz, CDCl₃) δ 8.98 (d, *J* = 9.6 Hz, 1H), 8.65 (s, 1H), 8.09 (d, *J* = 1.0 Hz, 1H), 8.08 (dd, *J* = 9.6, 1.6 Hz, 1H), 5.58 (hept, *J* = 6.7 Hz, 1H, CH-(CH₃)₂), 3.56 – 3.46 (m, 1H, CH-(CH₃)₂), 1.73 (d, *J* = 6.7 Hz, 6H, CH-(CH₃)₂), 1.54 (d, *J* = 6.8 Hz, 6H, CH-(CH₃)₂).

^{13}C NMR (151 MHz, CDCl_3) δ 138.70, 135.15, 128.78, 124.29, 122.23 (q, $J = 35.8$ Hz, CF_3), 119.68, 115.43, 52.19, 24.42, 22.87, 20.63.

^{19}F NMR (470 MHz, CDCl_3) δ -62.91

ESI-HRMS (m/z): Calc. for $\text{C}_{14}\text{H}_{18}\text{F}_3\text{N}_2^+$: 271.14; found 271.13962.

1,3-diisopropyl-6-methoxyimidazol[1,2-*a*]pyridinium iodide



Prepared following the general procedure above using 3-isopropyl-6-methoxyimidazo[1,2-*a*]pyridinium bromide (2.0 g, 7.4 mmol, 1.0 eq.), 2-iodopropane (6.1 mL, 31 mmol, 4.3 eq.). The product was obtained after drying *in vacuo* for 18 h (1.7 g, 24%).

^1H NMR (500 MHz, CDCl_3) δ 8.45 (d, $J = 7.5$ Hz, 1H), 7.82 (d, $J = 2.4$ Hz, 1H), 7.38 (d, $J = 1.0$ Hz, 1H), 7.08 (dd, $J = 7.6, 2.4$ Hz, 1H), 5.60 (hept, $J = 6.7$ Hz, 1H, $\text{CH}-(\text{CH}_3)_2$), 4.20 (s, 3H, $\text{O}-\text{CH}_3$), 3.43 – 3.34 (m, 1H, $\text{CH}-(\text{CH}_3)_2$), 1.59 (d, $J = 6.6$ Hz, 6H, $\text{CH}-(\text{CH}_3)_2$), 1.41 (d, $J = 6.8$ Hz, 6H, $\text{CH}-(\text{CH}_3)_2$).

^{13}C NMR (126 MHz, CDCl_3) δ 163.90, 141.20, 132.80, 127.16, 127.11, 115.20, 112.31, 92.22, 59.51, 50.39, 24.08, 22.70, 20.86.

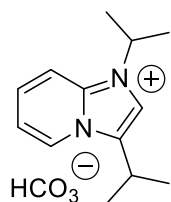
ESI-HRMS (m/z): Calc. for $\text{C}_{14}\text{H}_{21}\text{N}_2\text{O}^+$: 233.17; found 233.16324.

General procedure for the preparation of 1,3-diisopropylimidazol[1,2-*a*]pyridinium hydrogen carbonates

Using a modified and previously described procedure,¹ 1,3-diisopropyl-1*H*-imidazol[1,2-*a*]pyridine-4-ium hydrogen carbonate can be prepared from either iodide or triflate salt precursors. A representative procedure using the iodide salt is given below.

1,3-diisopropyl-1*H*-imidazol[1,2-*a*]pyridine-4-ium iodide salt (1 eq.) was dissolved in 10 mL of methanol and added to freshly prepared HCO_3^- resin (3 eq.). The pale yellow mixture was stirred for 30 minutes before removing the resin by vacuum filtration. The resin was washed with methanol (3 times) before discarding. The methanolic filtrate was dried under a stream of air overnight to afford a pale yellow coloured solid. The solids were treated by sonication/trituration in acetone (1 x 10 mL) and diethyl ether (2 x 10 mL), removing the yellow coloured supernatant each time before drying *in vacuo* to give the desired product as a colourless powder

1,3-diisopropyl-1*H*-imidazol[1,2-*a*]pyridine-4-ium hydrogen carbonate ($\text{MIC}^{\text{ipr}} \cdot \text{H}_2\text{CO}_3$)



Prepared following the general procedure above using 1,3-diisopropylimidazol[1,2-*a*]pyridinium iodide (0.4 g, 1.2 mmol, 1 eq.), HCO₃⁻ resin (4.8 mL, 3 eq.). The product was obtained after drying *in vacuo* for 18 h. Elemental analysis and thermogravimetric analysis indicate that the product was obtained as a monohydrate. (0.22 g, 78 %).

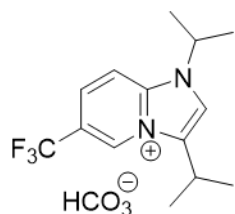
¹H NMR (600 MHz, MeOD) δ 8.78 (dt, *J* = 6.9, 1.1 Hz, 1H), 8.15 (dt, *J* = 9.3, 1.1 Hz, 1H), 8.10 (d, *J* = 1.0 Hz, 1H), 8.01 (ddd, *J* = 9.3, 7.0, 1.1 Hz, 1H), 7.55 (td, *J* = 6.9, 1.1 Hz, 1H), 5.09 (hept, *J* = 6.7 Hz, 1H, CH-(CH₃)₂), 3.47 (pd, *J* = 6.9, 1.0 Hz, 1H, CH-(CH₃)₂), 1.64 (d, *J* = 6.7 Hz, 6H, CH-(CH₃)₂), 1.47 (d, *J* = 6.9 Hz, 6H, CH-(CH₃)₂).

¹³C NMR (151 MHz, MeOD) δ 160.03, 138.72, 133.94, 132.83, 126.69, 116.96, 110.85, 50.03, 23.66, 20.87, 19.37.

Anal. calc. for C₁₄H₂₀N₂O₃ (+ H₂O): C, 59.56; H, 7.85; N, 9.92. Found: C, 59.49; H, 7.83; N, 9.92.

ESI-HRMS (*m/z*): Calc. for C₁₃H₁₉N₂⁺: 203.1543; found 203.15376.

1,3-diisopropyl-6-trifluoromethylimidazol[1,2-*a*] pyridine-4-ium hydrogen carbonate (CF₃-NHC^{IPr}•H₂CO₃)



Prepared following the general procedure above using 1,3-diisopropyl-6-trifluoromethylimidazol[1,2-*a*]pyridinium iodide (0.4 g, 1.0 mmol, 1 eq.), HCO₃⁻ resin (4.0 mL, 3 eq.). Product was obtained after drying *in vacuo* for 18 h. (0.18 g, 53 %).

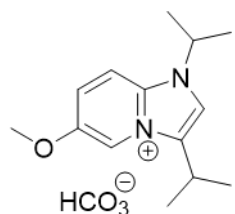
¹H NMR (500 MHz, MeOD) δ 9.24 (s, 1H), 8.36 (d, *J* = 9.6 Hz, 1H), 8.29 (s, 1H), 8.22 (dd, *J* = 9.5, 1.6 Hz, 1H), 5.16 (p, *J* = 6.7 Hz, 1H, CH-(CH₃)₂), 3.59 (h, *J* = 6.6 Hz, 1H, CH-(CH₃)₂), 1.66 (d, *J* = 6.6 Hz, 6H, CH-(CH₃)₂), 1.47 (d, *J* = 6.8 Hz, 6H, CH-(CH₃)₂).

¹³C NMR (126 MHz, MeOD) δ 166.44, 140.58, 137.27, 129.65, 127.59, 125.18, 122.56(q, *J* = 34.9 Hz, CF₃), 119.96, 113.77, 52.22, 24.92, 22.25, 20.96.

¹⁹F NMR (470 MHz, CDCl₃) δ -63.49.

ESI-HRMS (*m/z*): Calc. for C₁₄H₁₈F₃N₂⁺: 271.14; found 271.13977.

1,3-diisopropyl-6-methoxyimidazol[1,2-*a*] pyridine-4-ium hydrogen carbonate



Prepared following the general procedure above using 1,3-diisopropylimidazol[1,2-*a*]pyridinium iodide (0.4 g, 1.2 mmol, 1 eq.), HCO₃⁻ resin (4.8 mL, 3 eq.). The product was obtained after drying *in vacuo* for 18 h. (0.12 g, 36 %).

^1H NMR (600 MHz, MeOD) δ 8.58 (dd, $J = 7.6, 2.0$ Hz, 1H), 7.87 (d, $J = 1.0$ Hz, 1H), 7.45 (d, $J = 2.6$ Hz, 1H), 7.17 (dd, $J = 7.6, 2.4$ Hz, 1H), 5.05 – 4.97 (m, 1H, $\text{CH}-(\text{CH}_3)_2$), 4.10 (d, $J = 1.3$ Hz, 3H, $\text{O}-\text{CH}_3$), 3.38 (p, $J = 6.7$ Hz, 1H, $\text{CH}-(\text{CH}_3)_2$), 1.62 (d, $J = 6.6$ Hz, 6H, $\text{CH}-(\text{CH}_3)_2$), 1.45 (d, $J = 6.8$ Hz, 6H, $\text{CH}-(\text{CH}_3)_2$).

^{13}C NMR (151 MHz, MeOD) δ 163.91, 141.14, 132.94, 127.44, 115.38, 110.84, 89.59, 56.30, 49.22, 23.52, 20.67, 19.51.

ESI-HRMS (m/z): Calc. for $\text{C}_{14}\text{H}_{21}\text{N}_2\text{O}^+$: 233.17; found 233.16304.

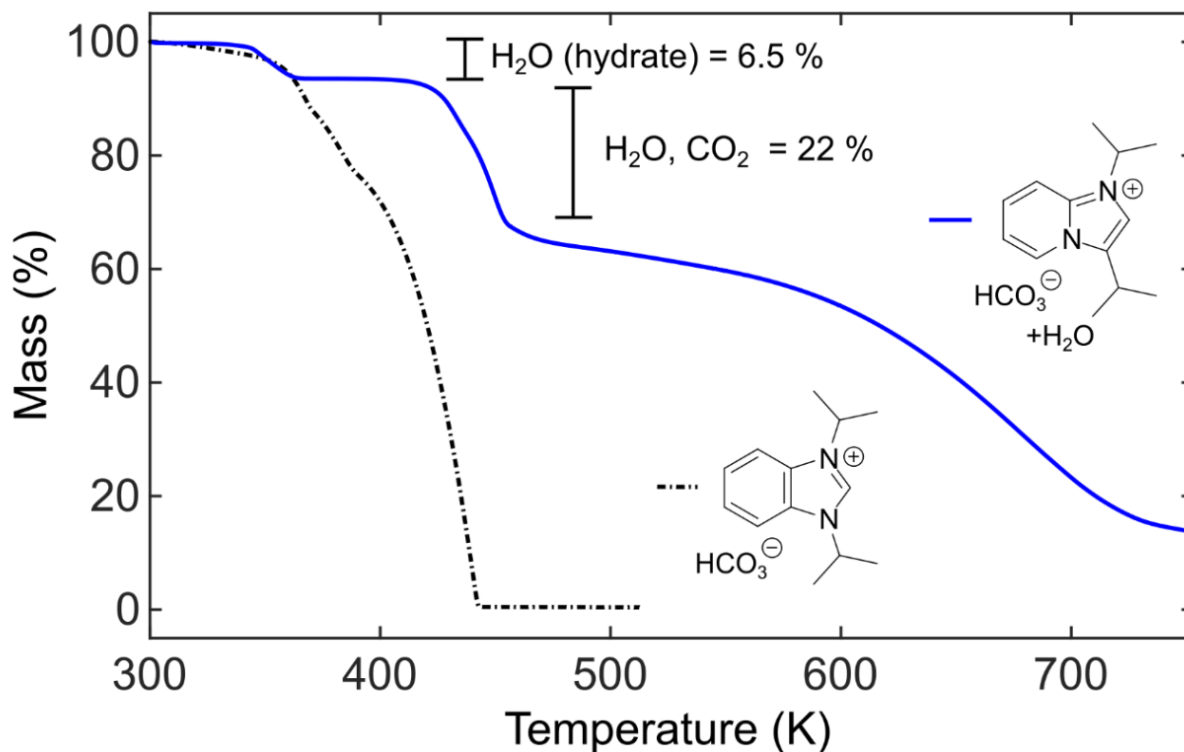
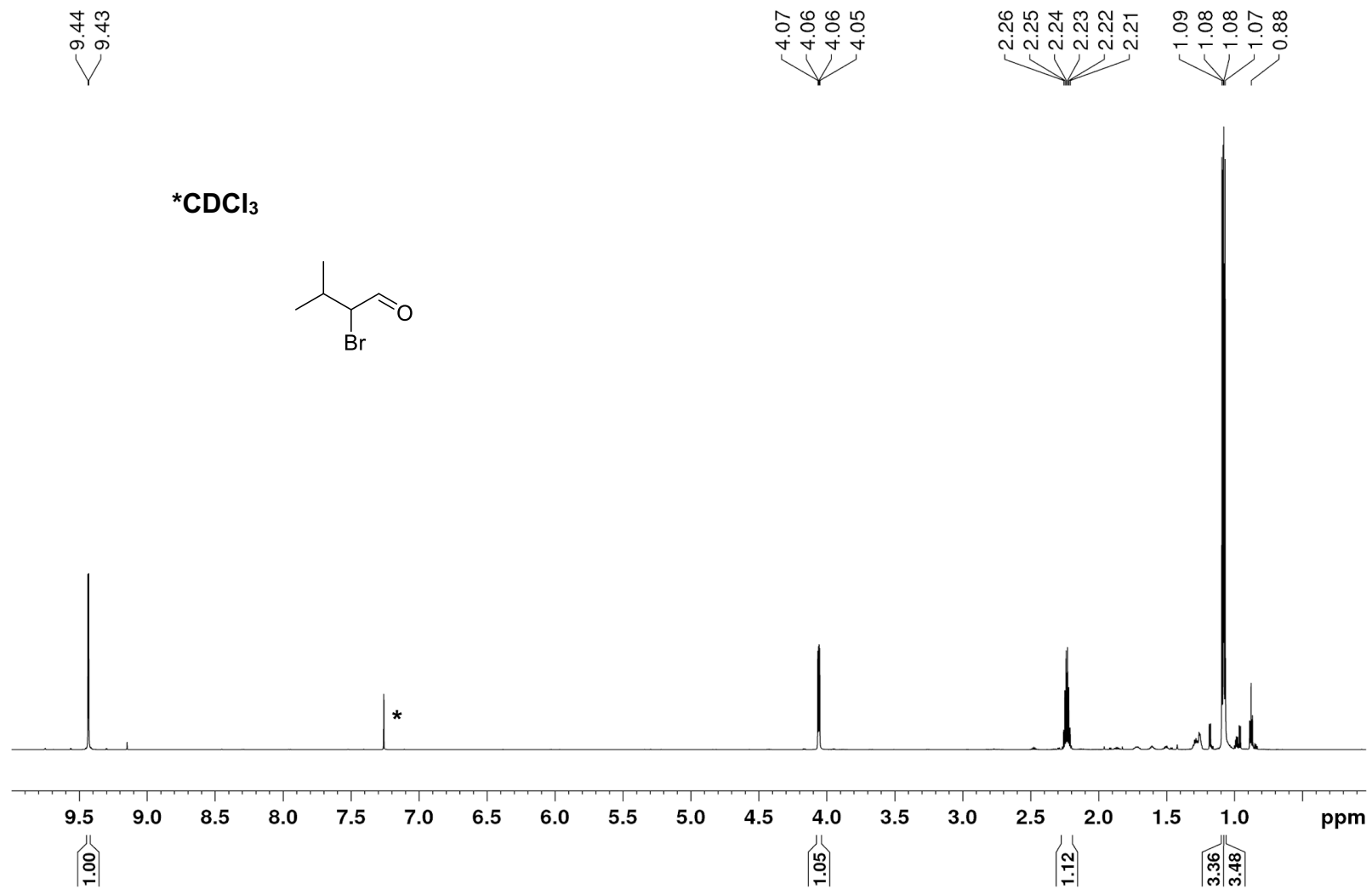


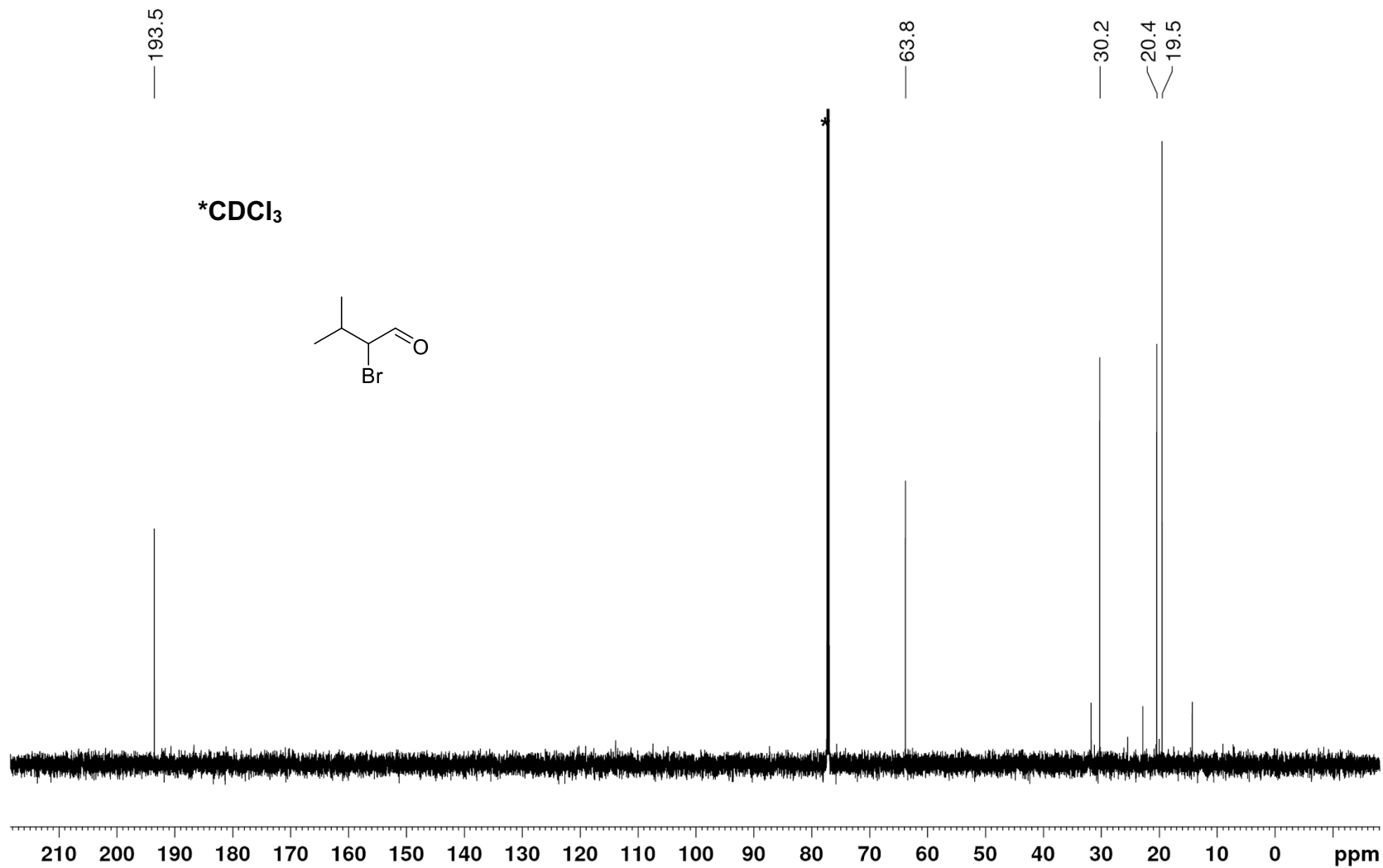
Figure S1: TGA curves for $\text{MIC}^{\text{iPr}} \cdot \text{H}_2\text{CO}_3$ (solid, blue) and $\text{NHC}^{\text{iPr}} \cdot \text{H}_2\text{CO}_3$ (dashed, black); ramp: $10^\circ\text{C min}^{-1}$, mass loading: 10 ± 2 mg.

Figure S2: ^1H , ^{13}C $\{^1\text{H}\}$, ^{19}F $\{^1\text{H}\}$ NMR spectra

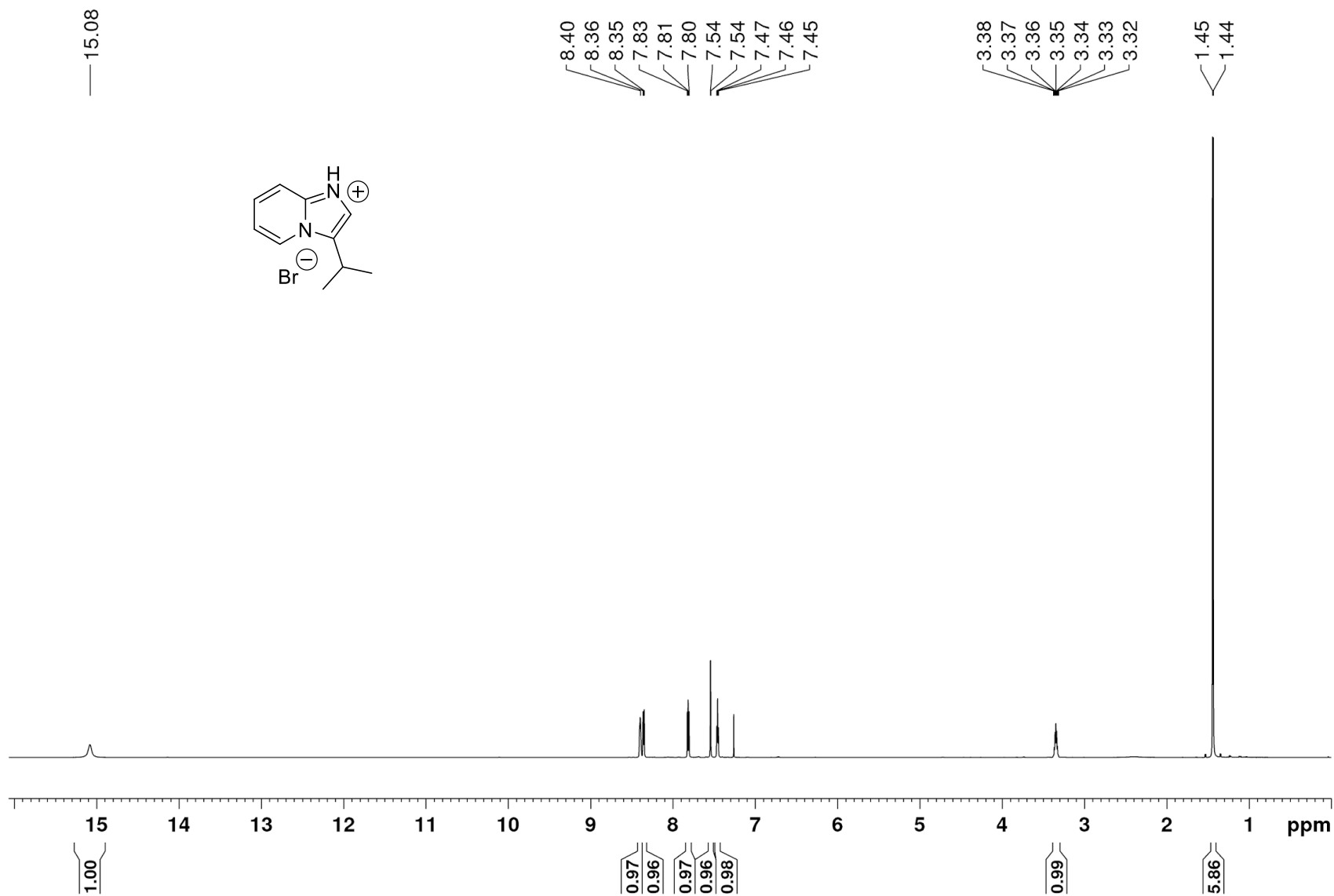
^1H NMR spectrum (700 MHz, CDCl_3) for 2-bromo-3-methylbutanal



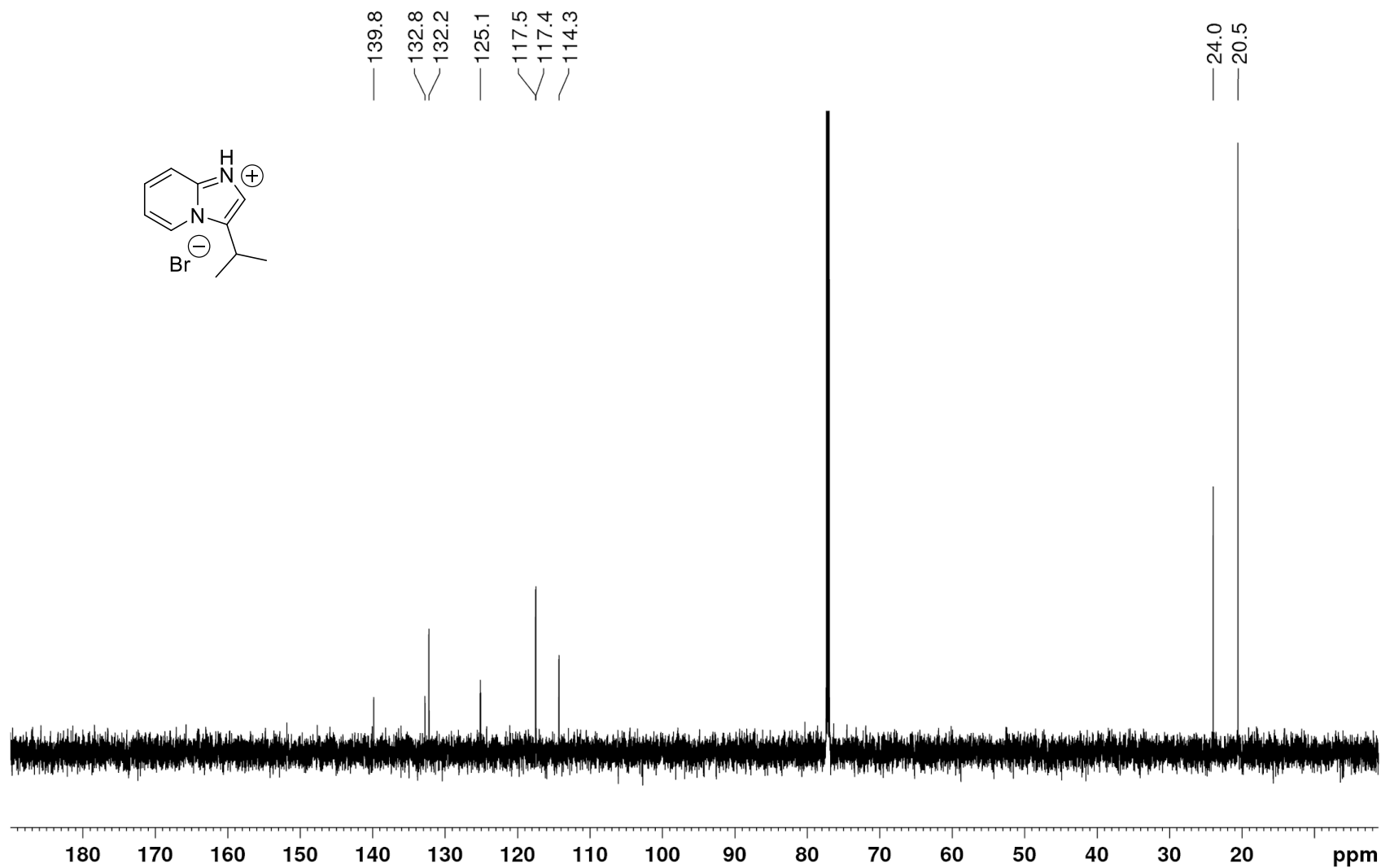
¹H NMR spectrum (700 MHz, CDCl₃) for 2-bromo-3-methylbutanal



¹H NMR spectrum for 3-isopropylimidazo[1,2-a]pyridin-1-ium bromide (700 MHz, CDCl₃)



¹³C {¹H} NMR spectrum for 3-isopropylimidazo[1,2-a]pyridin-1-ium bromide (175 MHz, CDCl₃)

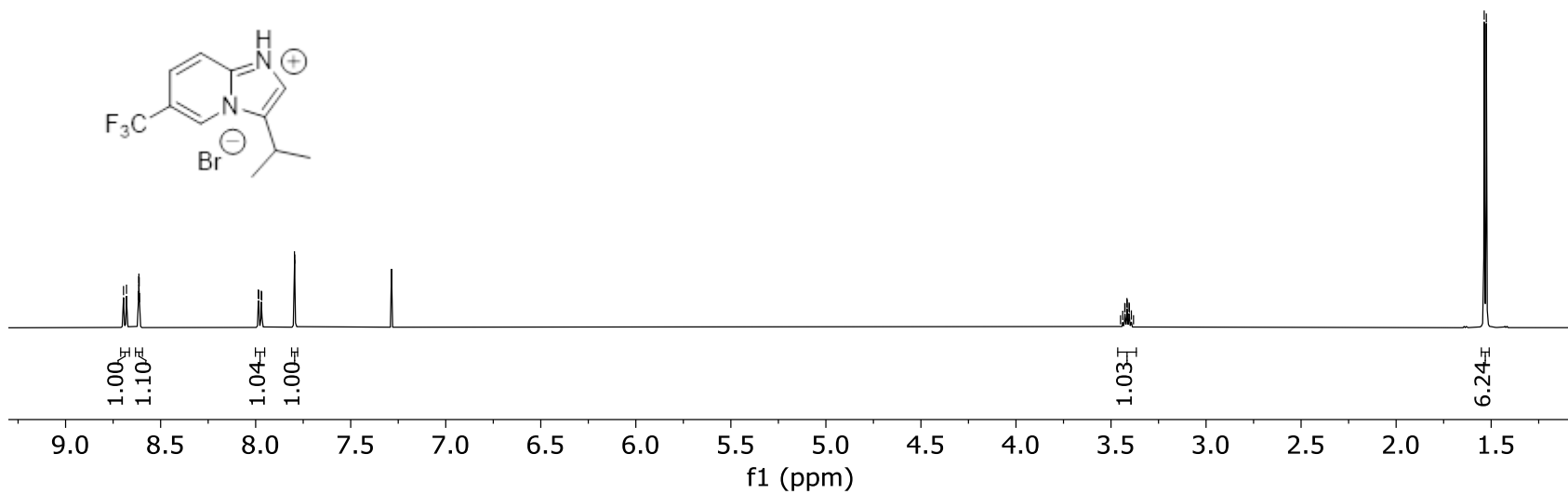
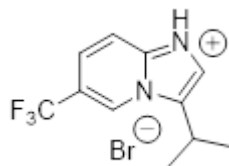


¹H NMR spectrum for 3-isopropyl-6-trifluoromethylimidazo[1,2-a]pyridinium bromide (500 MHz, CDCl₃)

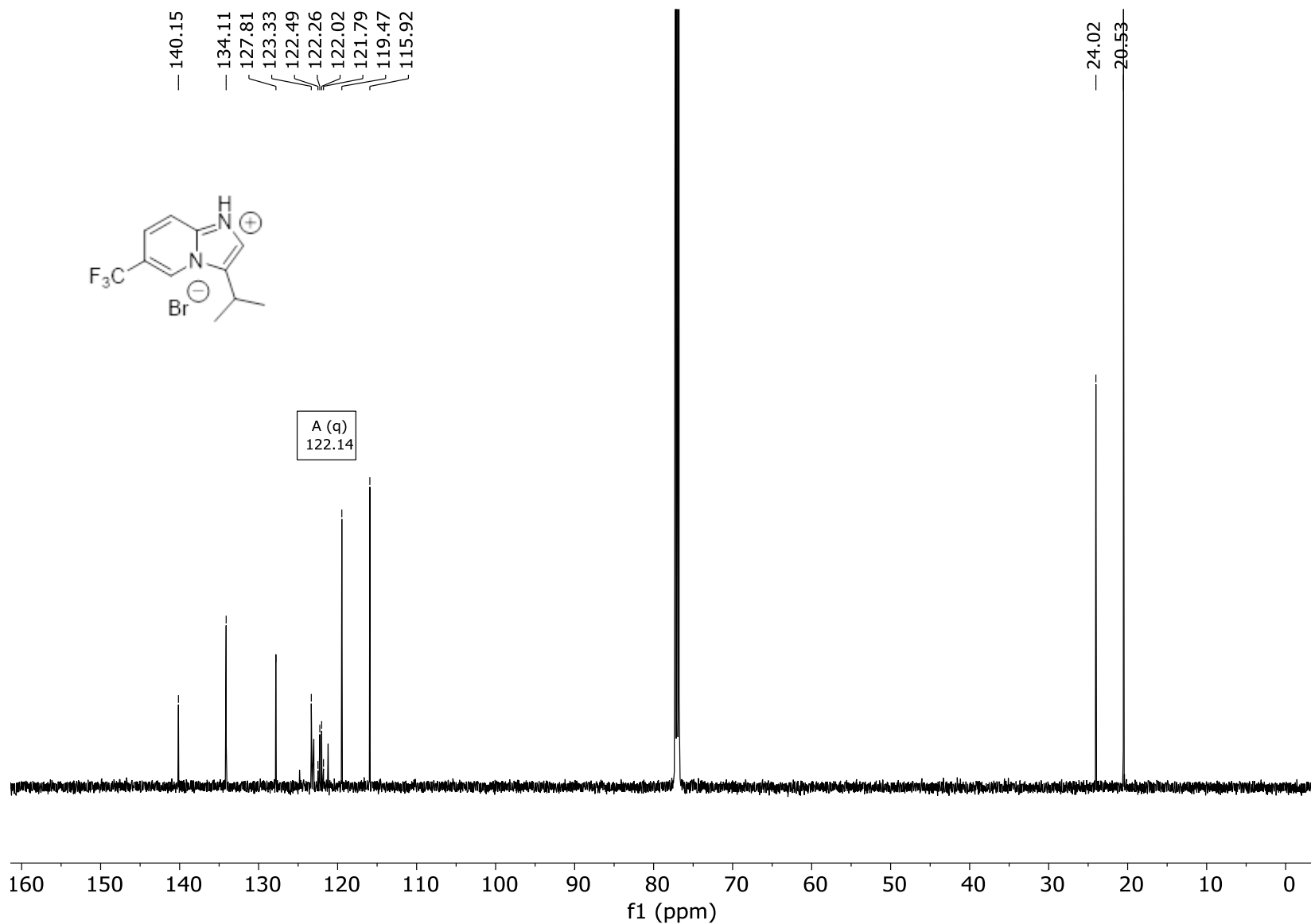
8.70
8.68
8.62
8.62
8.61
7.99
7.98
7.97
7.97
7.80
7.79

3.45
3.44
3.43
3.43
3.42
3.41
3.40
3.40
3.39
3.38

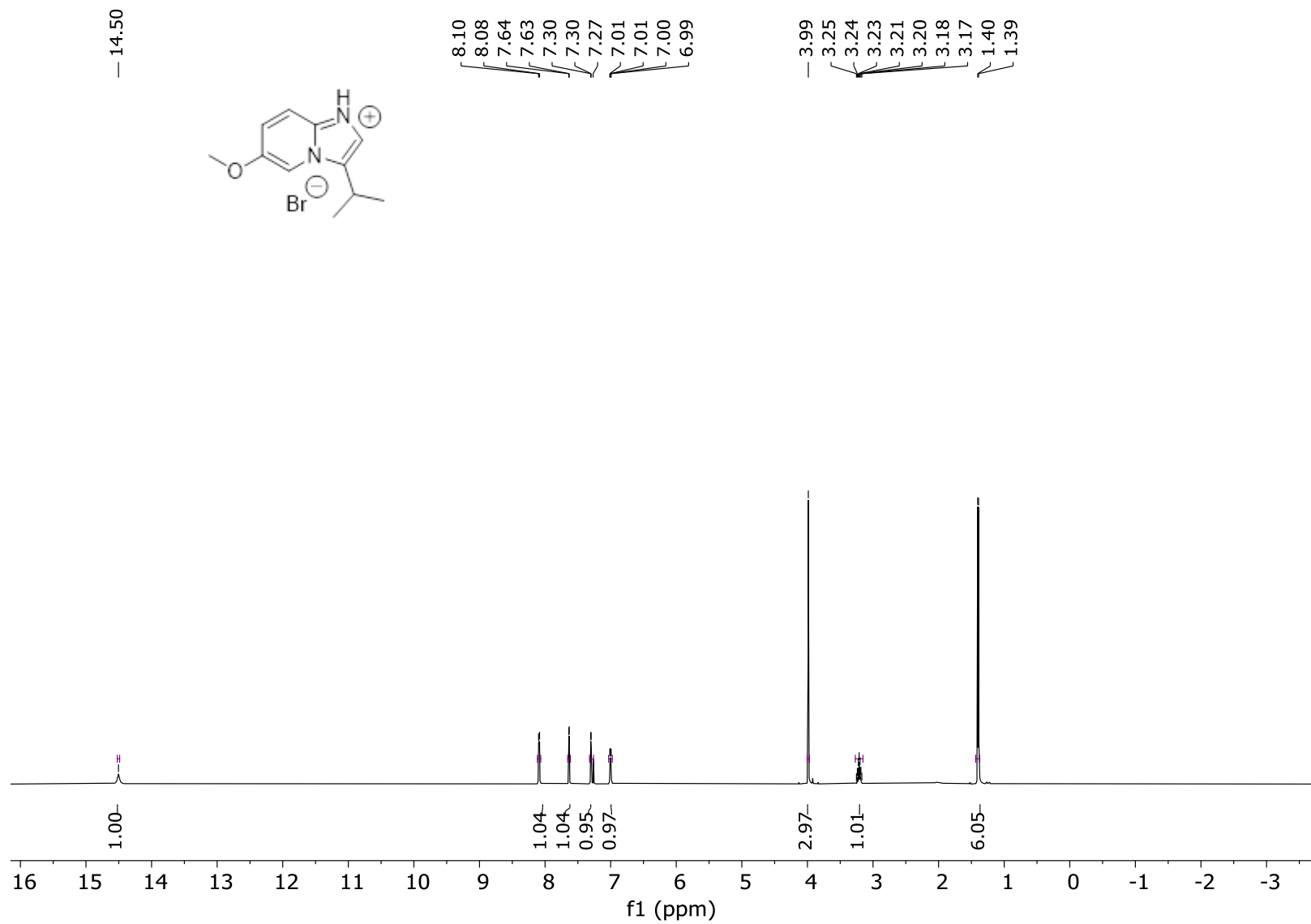
1.54
1.53



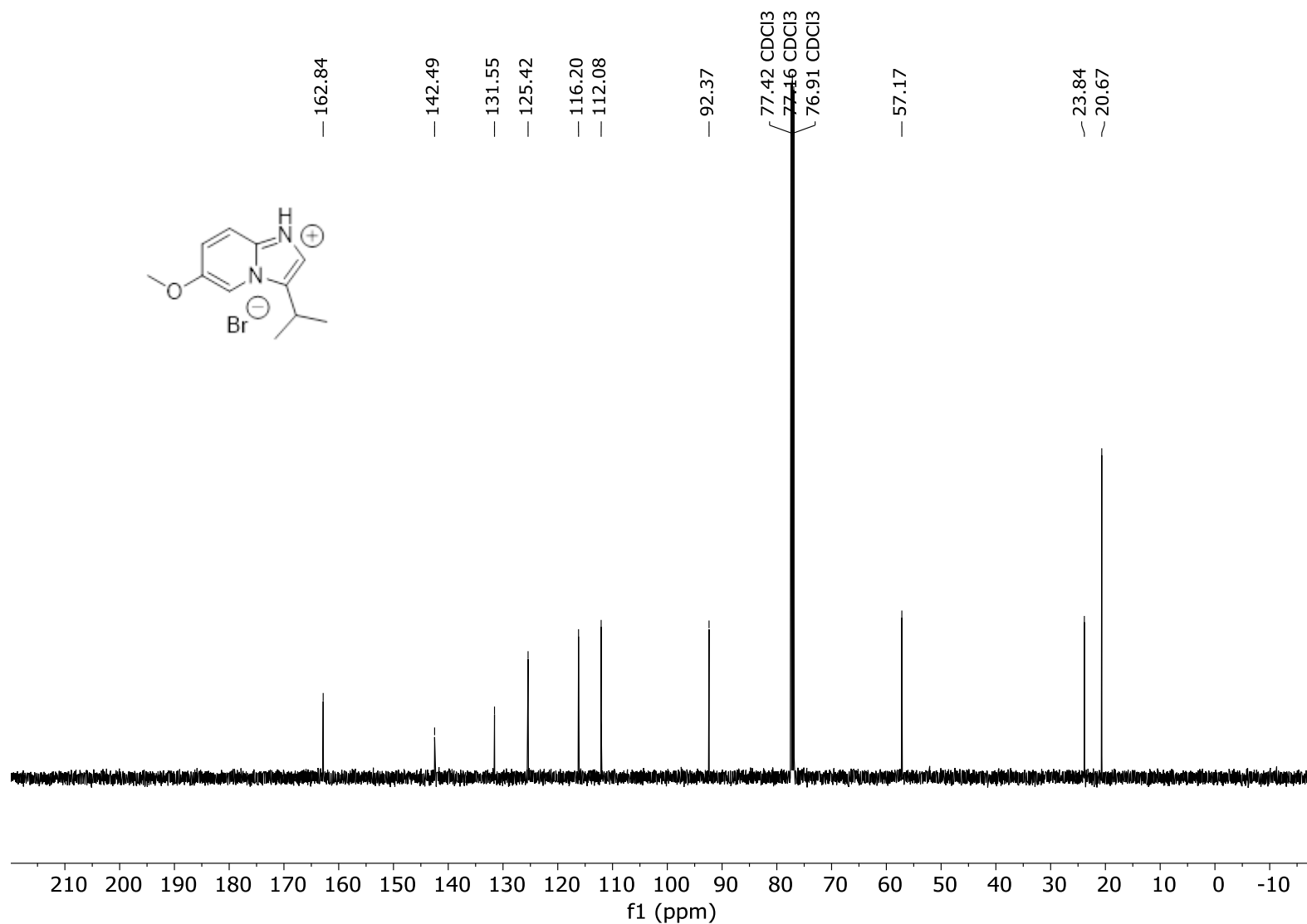
^{13}C $\{^1\text{H}\}$ NMR spectrum for 3-isopropyl-6-trifluoromethylimidazo[1,2-a]pyridinium bromide (126 MHz, CDCl_3)



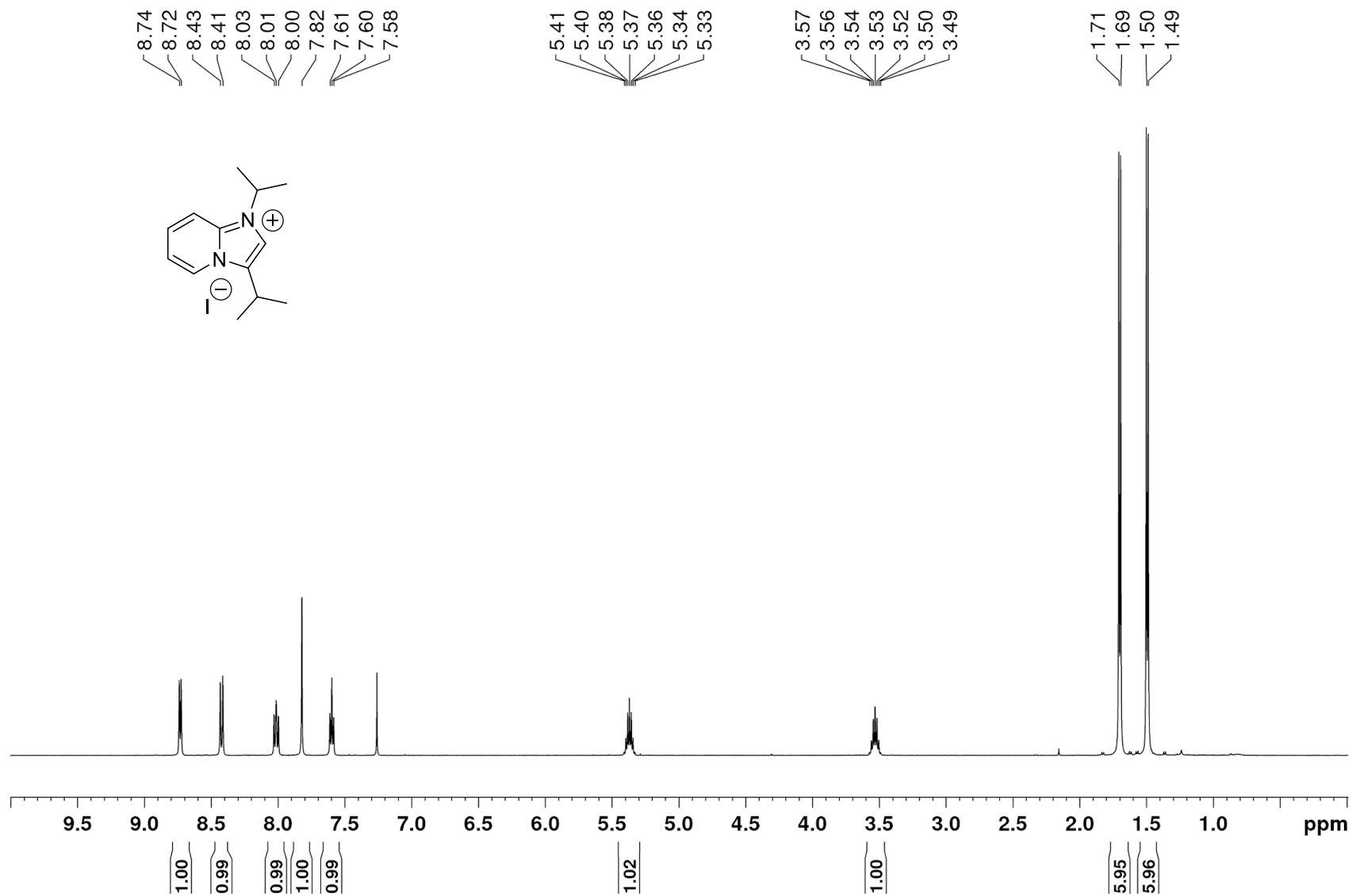
¹H NMR spectrum for 3-isopropyl-6-methoxyimidazo[1,2-a]pyridinium bromide (500 MHz, CDCl₃)



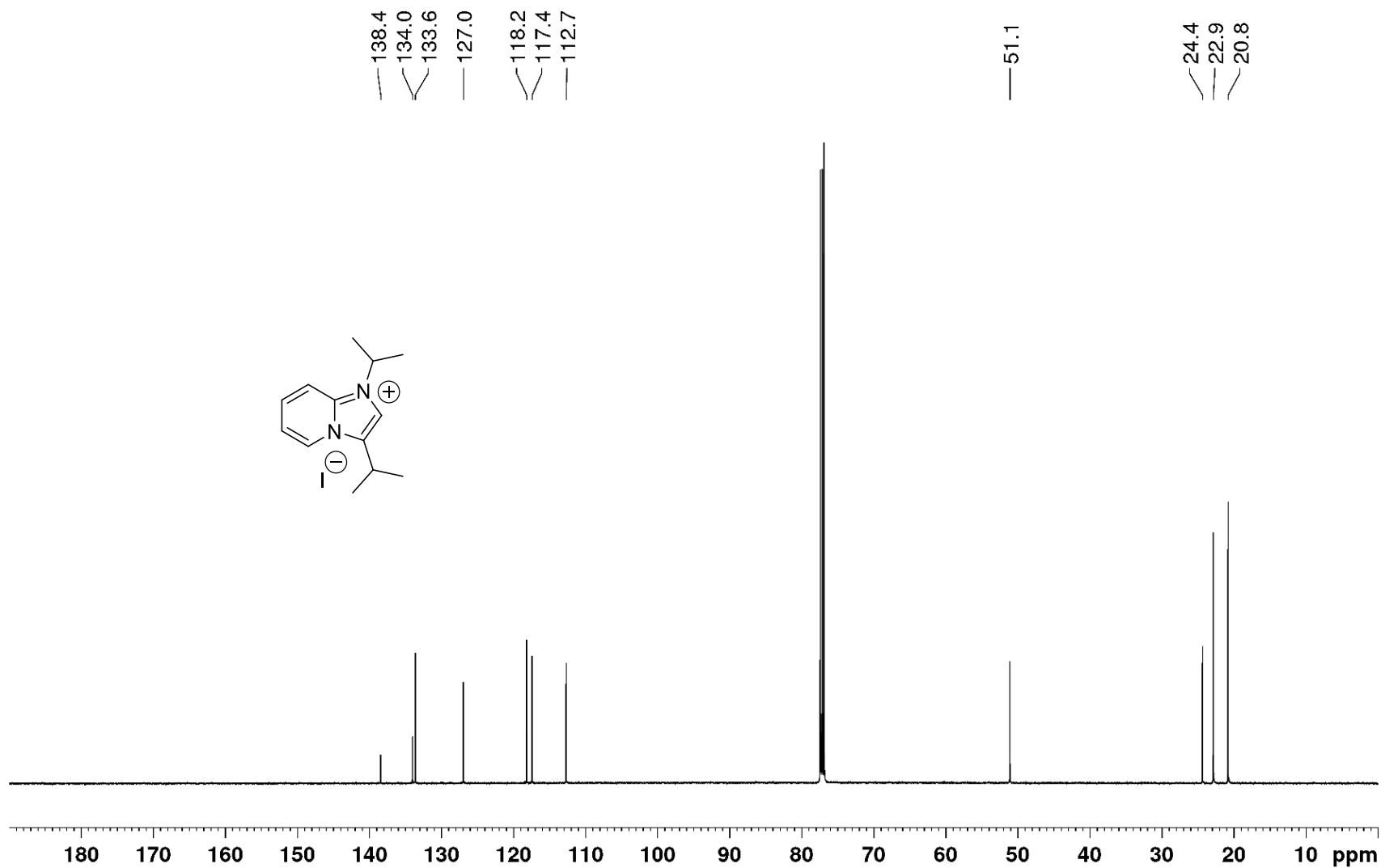
¹³C {¹H} NMR spectrum for 3-isopropyl-6-methoxyimidazo[1,2-a]pyridinium bromide (126 MHz, CDCl₃)



¹H NMR spectrum for 1,3-diisopropyl-1*H*-imidazol[1,2-*a*]pyridine-4-ium iodide (500 MHz, CDCl₃)



^{13}C $\{^1\text{H}\}$ NMR spectrum for 1,3-diisopropyl-1*H*-imidazol[1,2-*a*]pyridine-4-ium iodide (125 MHz, CDCl_3)



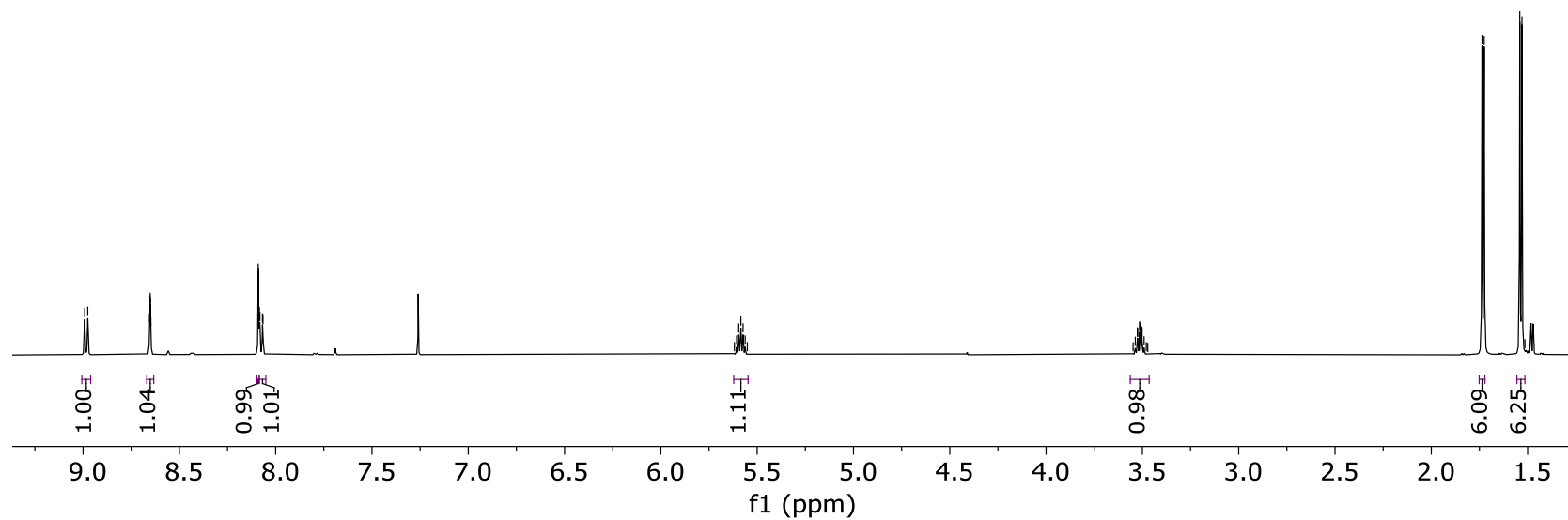
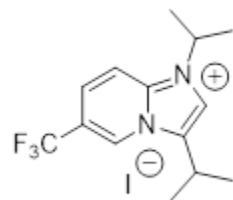
¹H NMR spectrum for 1,3-diisopropyl-6-trifluoromethylimidazol[1,2-*a*]pyridinium iodide (500 MHz, CDCl₃)

8.99
8.98
8.65
8.65
8.65
8.65
8.09
8.09
8.08
8.08
8.07
8.07

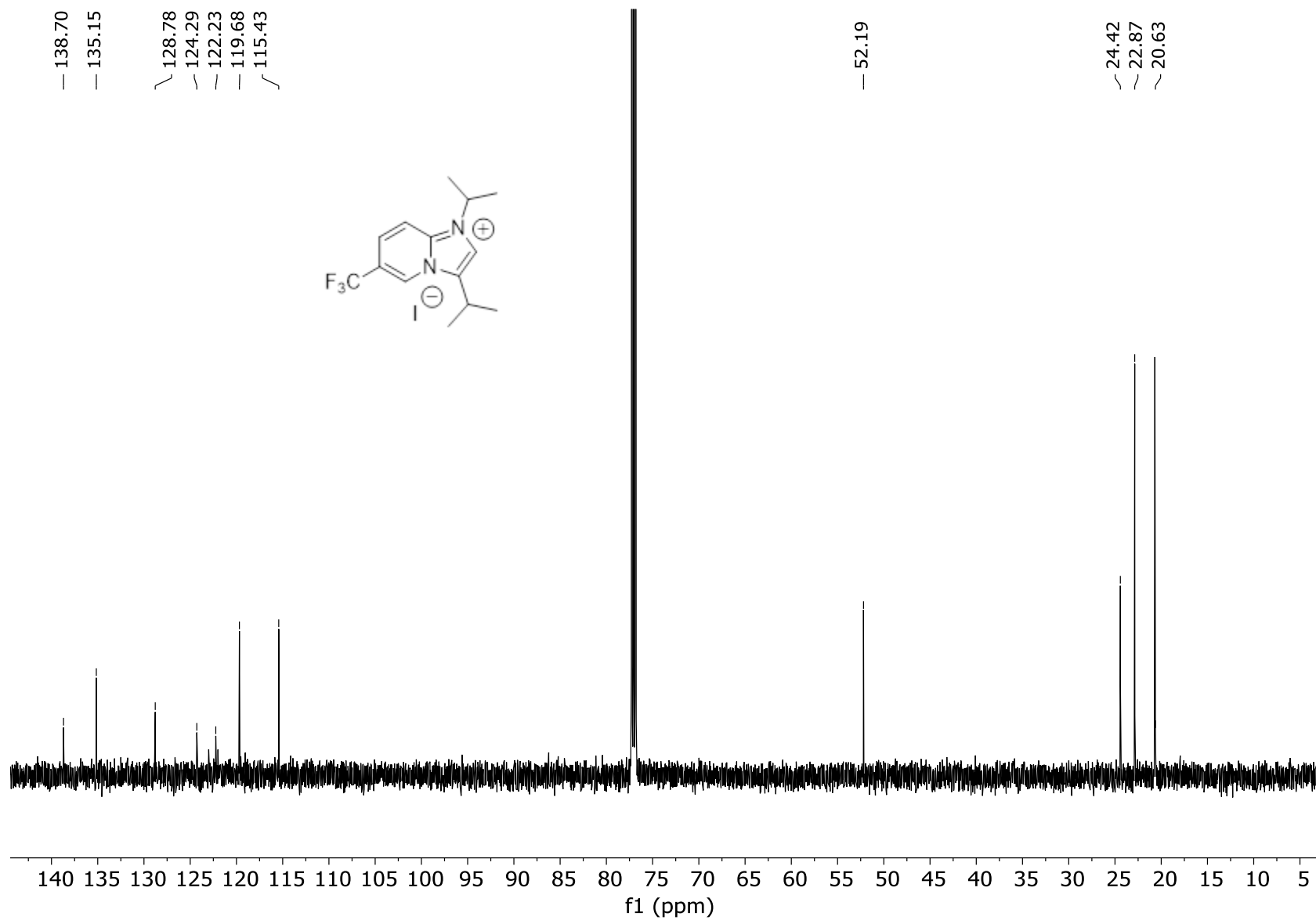
5.62
5.61
5.60
5.58
5.57
5.56
5.55

3.55
3.54
3.53
3.52
3.51
3.51
3.50
3.50
3.49
3.48
3.47

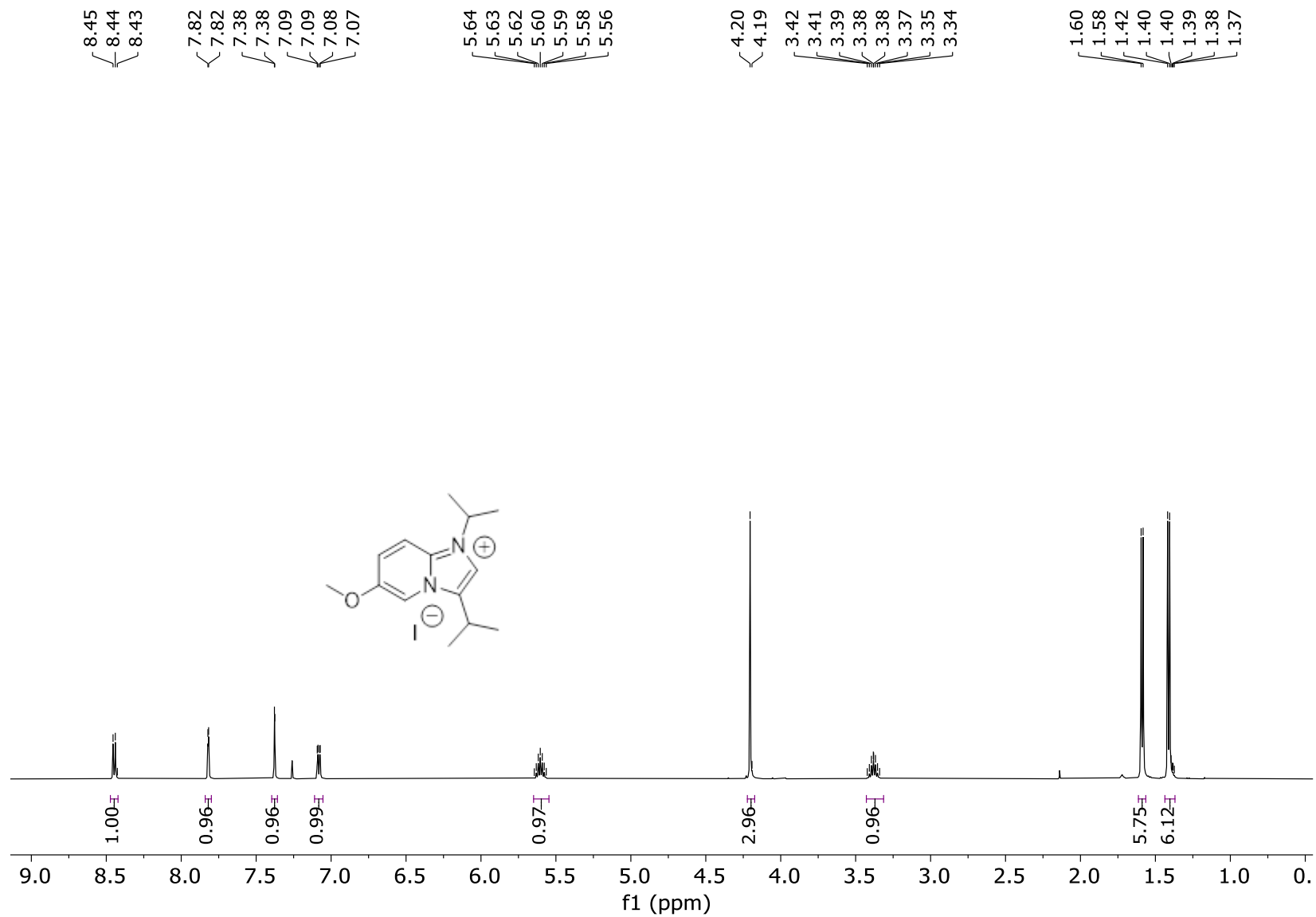
1.74
1.73
1.54
1.53
1.51



^{13}C $\{^1\text{H}\}$ NMR spectrum for 1,3-diisopropyl-6-trifluoromethylimidazol[1,2-*a*]pyridinium iodide (125 MHz, CDCl_3)



¹H NMR spectrum for 1,3-diisopropyl-6-methoxyimidazol[1,2-a]pyridinium iodide (500 MHz, CDCl₃)



8.45
8.44
8.43

7.82
7.82

7.38
7.38

7.09
7.09
7.08
7.07

5.64
5.63
5.62
5.60
5.59
5.58
5.56

4.20
4.19

3.42
3.41
3.39
3.38
3.38
3.37
3.35
3.34

1.60
1.58
1.42
1.40
1.40
1.39
1.38
1.37

1.00

0.96

0.96

0.99

0.97

2.96

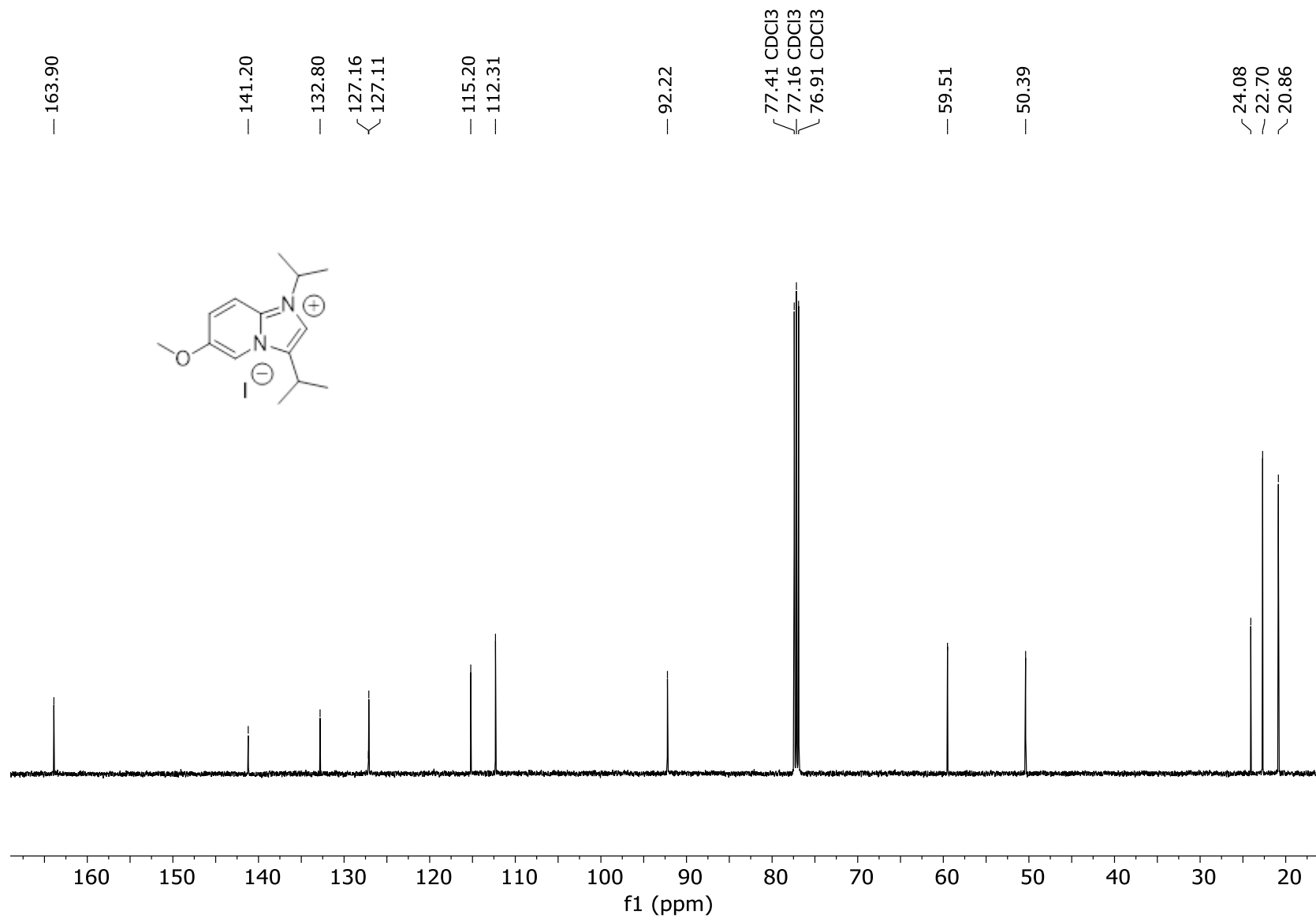
0.96

5.75

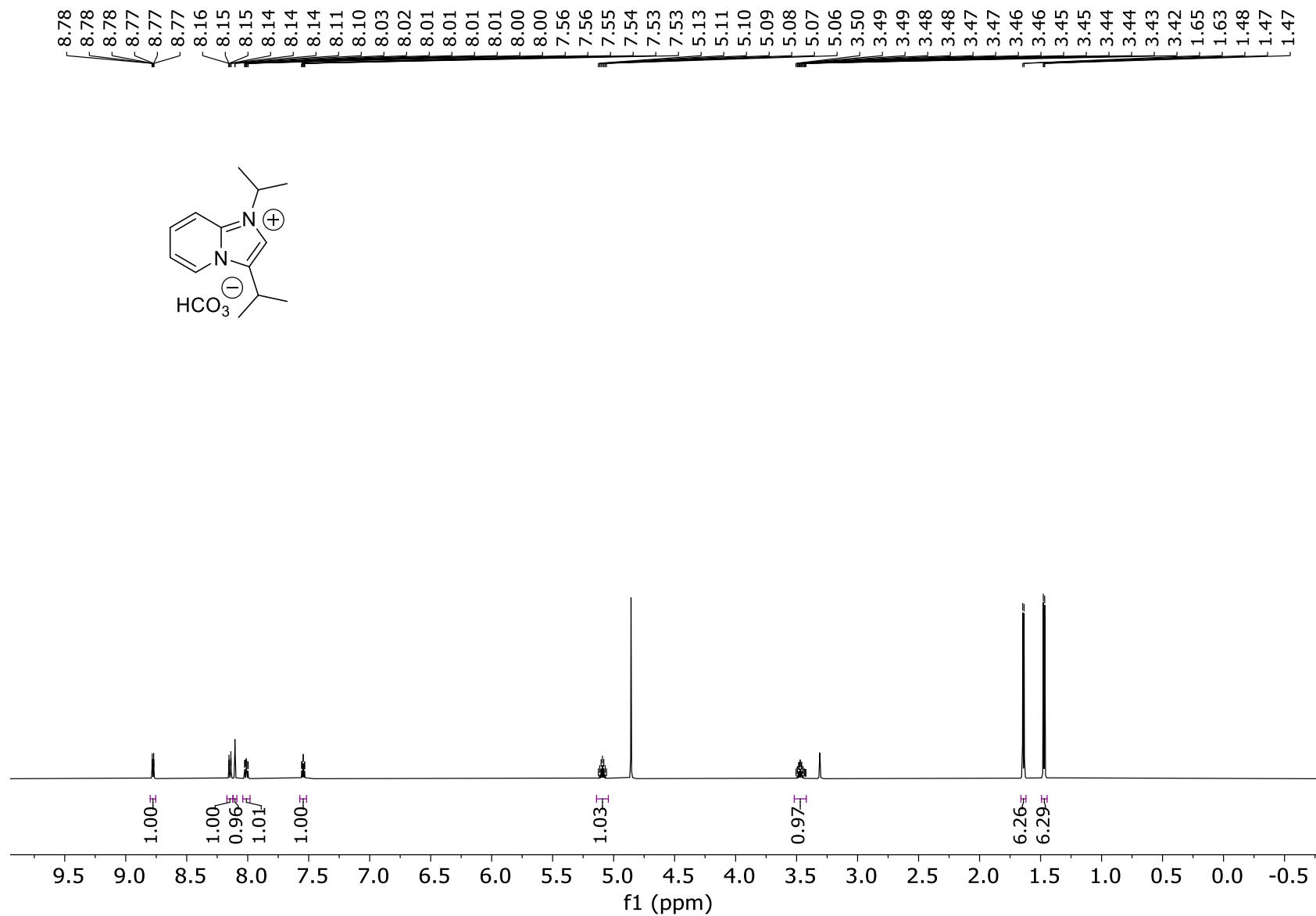
6.12

f1 (ppm)

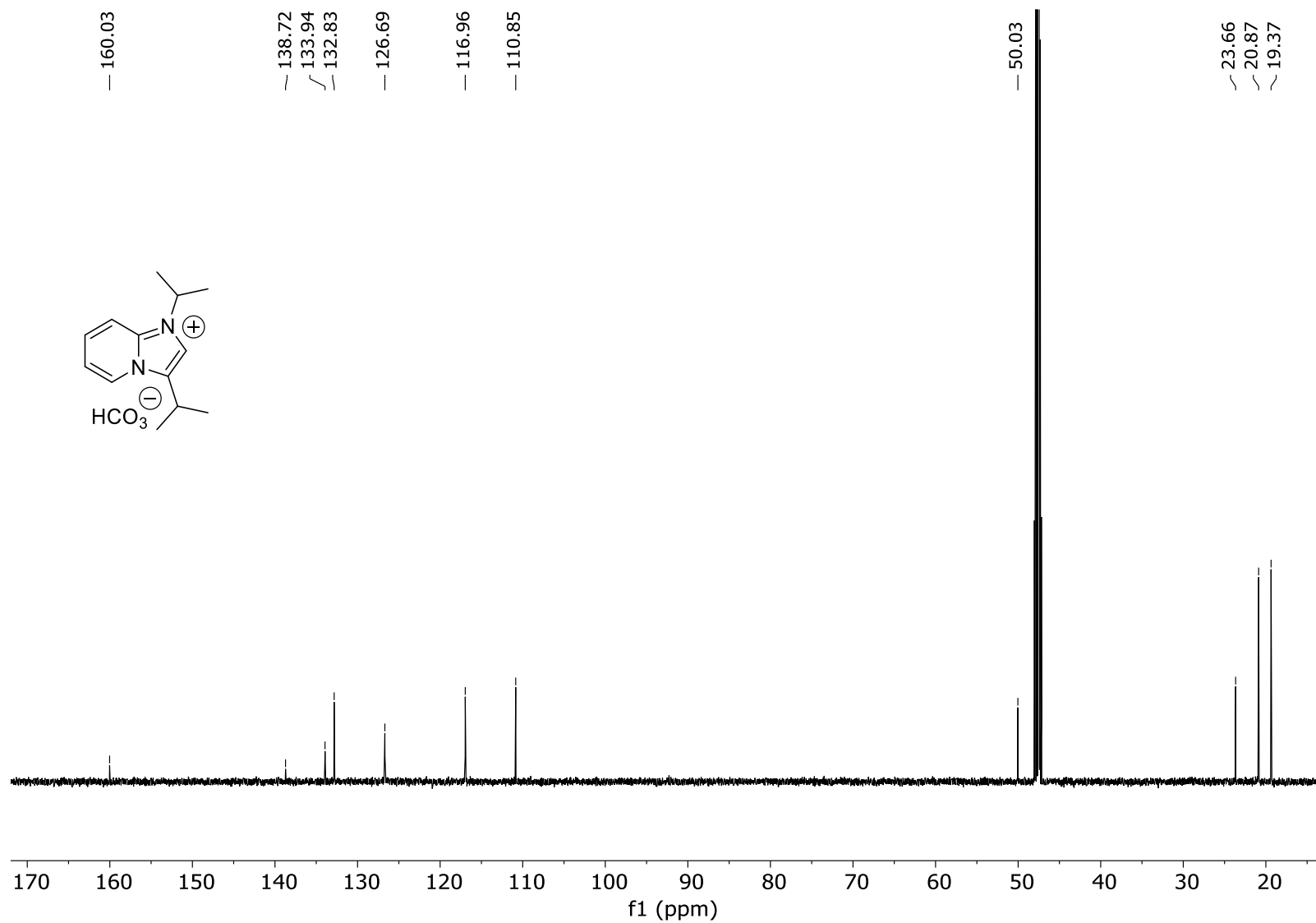
^{13}C { ^1H } NMR spectrum for 1,3-diisopropyl-6-methoxyimidazol[1,2-*a*]pyridinium iodide (125 MHz, CDCl_3)



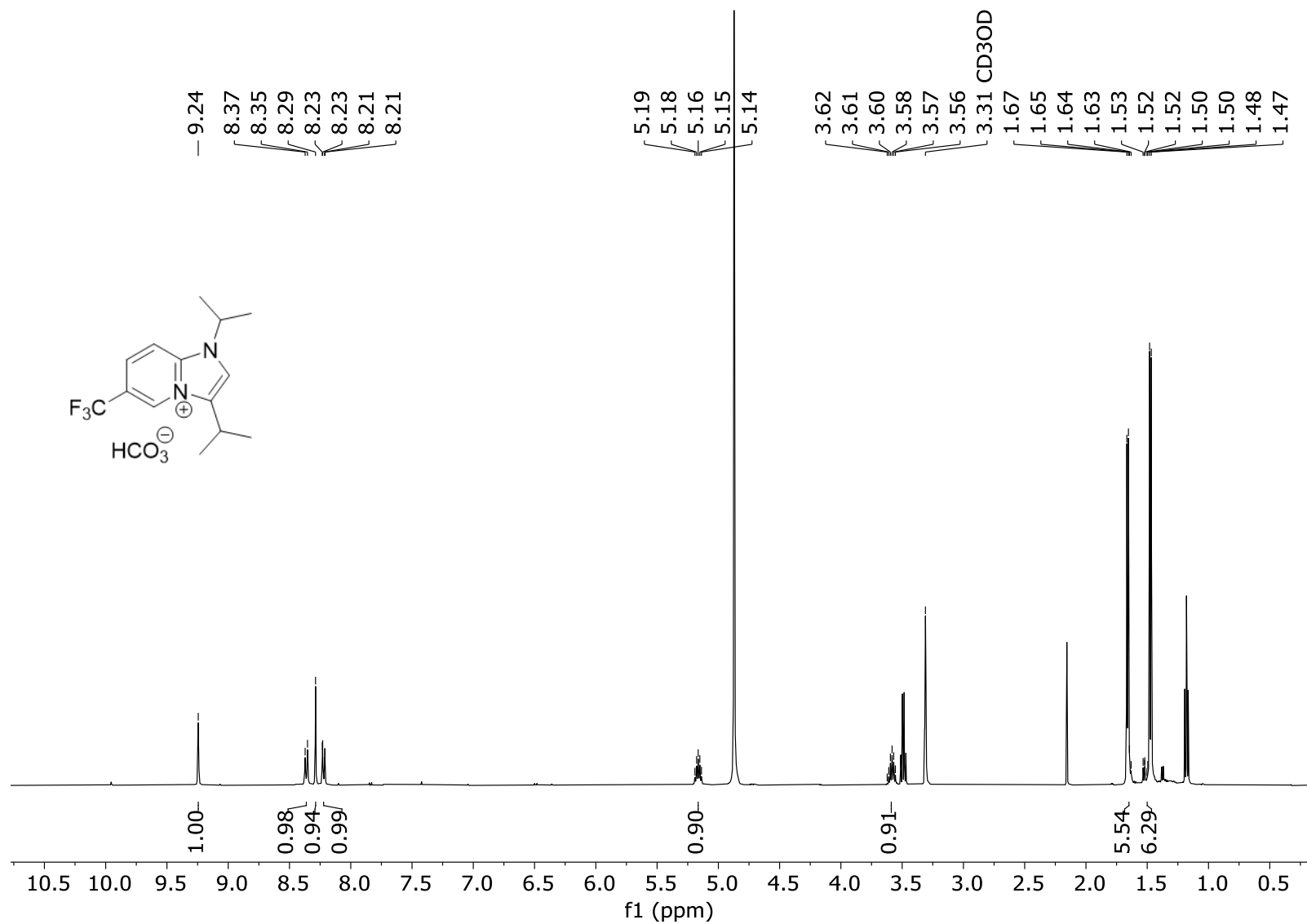
¹H NMR spectrum for 1,3-diisopropyl-1*H*-imidazol[1,2-*a*]pyridine-4-ium hydrogen carbonate (500 MHz, CD₃OD)



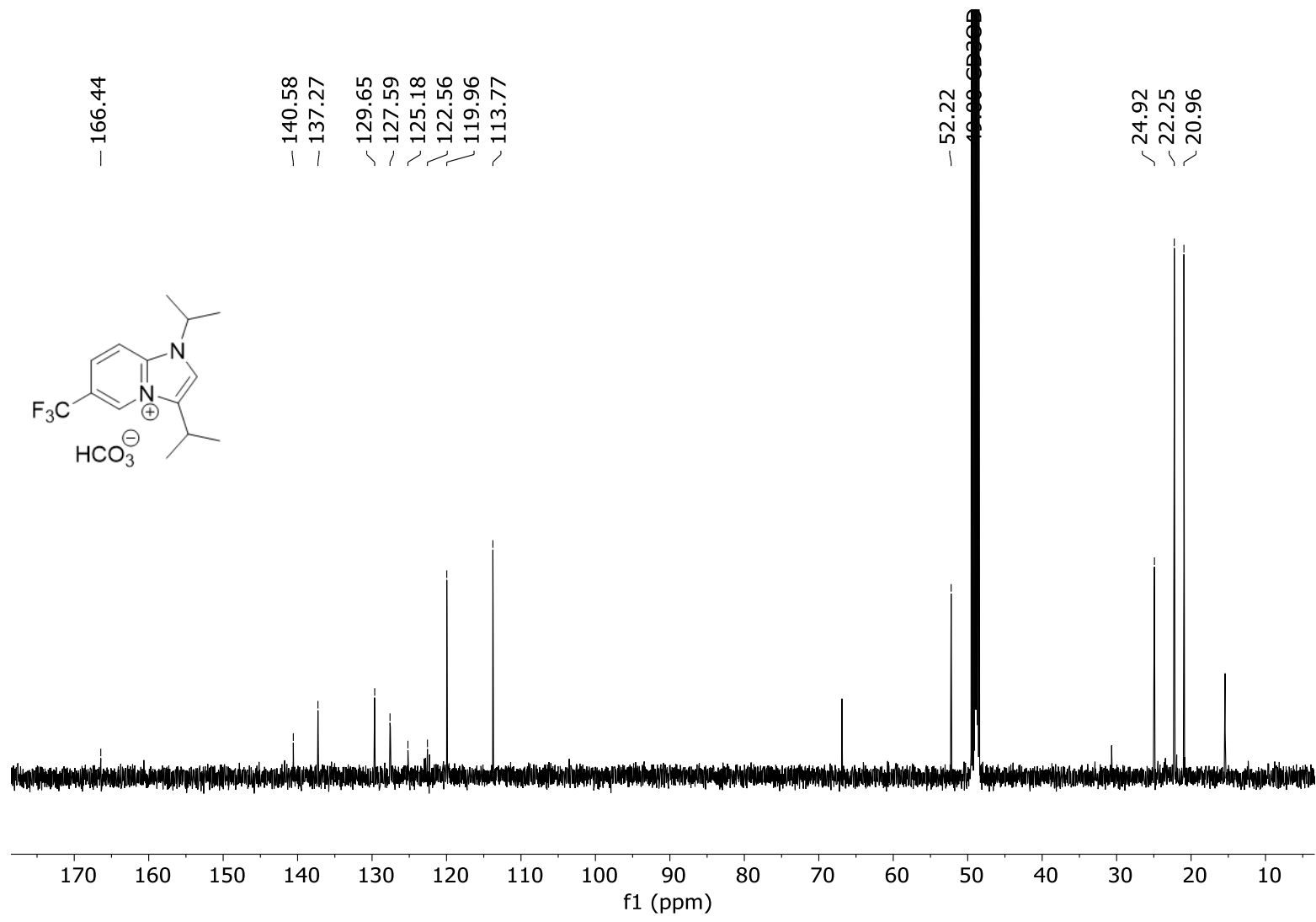
^{13}C $\{^1\text{H}\}$ NMR spectrum for 1,3-diisopropyl-1*H*-imidazol[1,2-*a*]pyridine-4-ium hydrogen carbonate (125 MHz, CD_3OD)



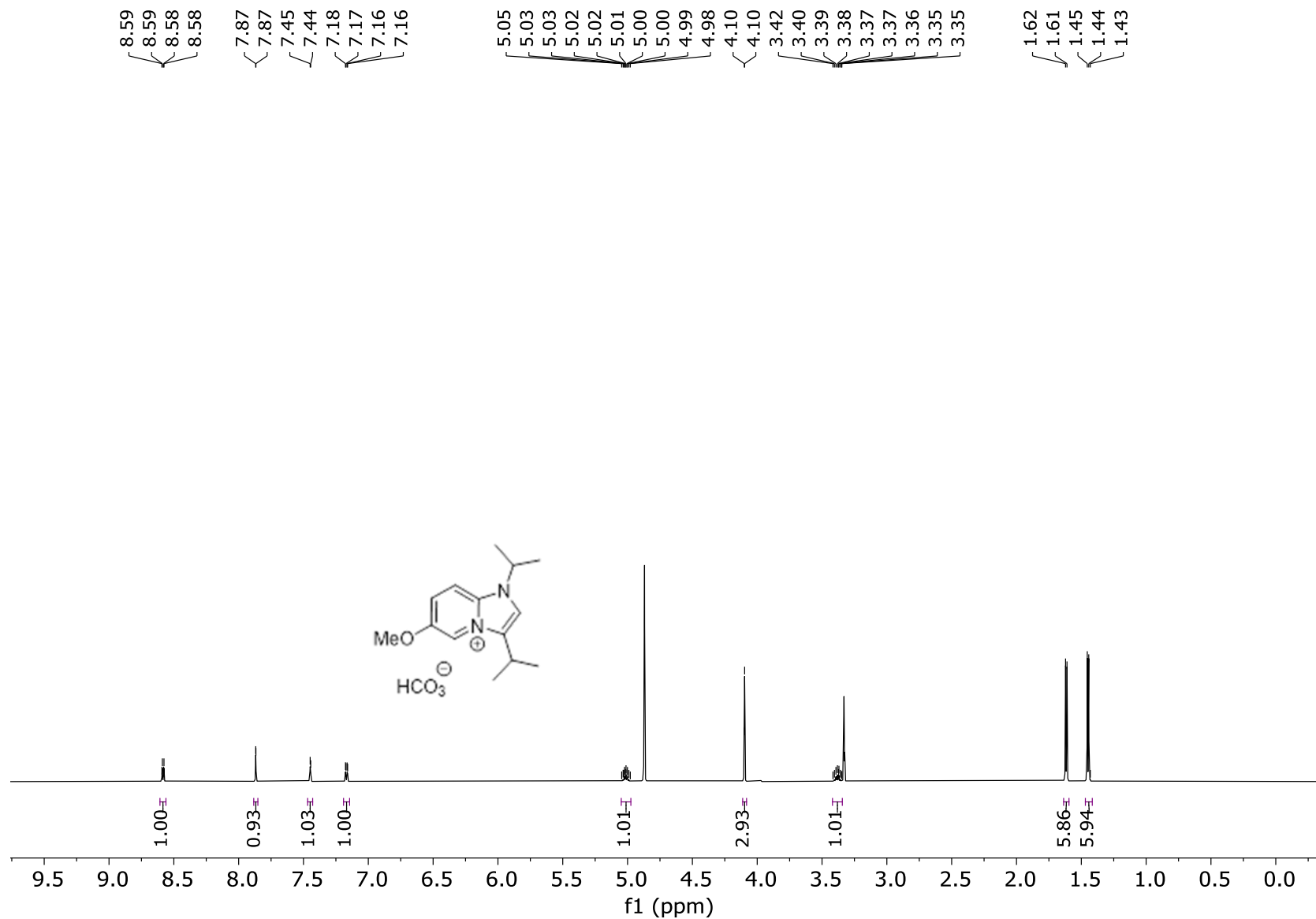
¹H NMR spectrum of 1,3-diisopropyl-6-trifluoromethylimidazol[1,2-a]pyridine-4-ium hydrogen carbonate (**CF₃-NHC^{iPr}•H₂CO₃**), 500 MHz, CD₃OD



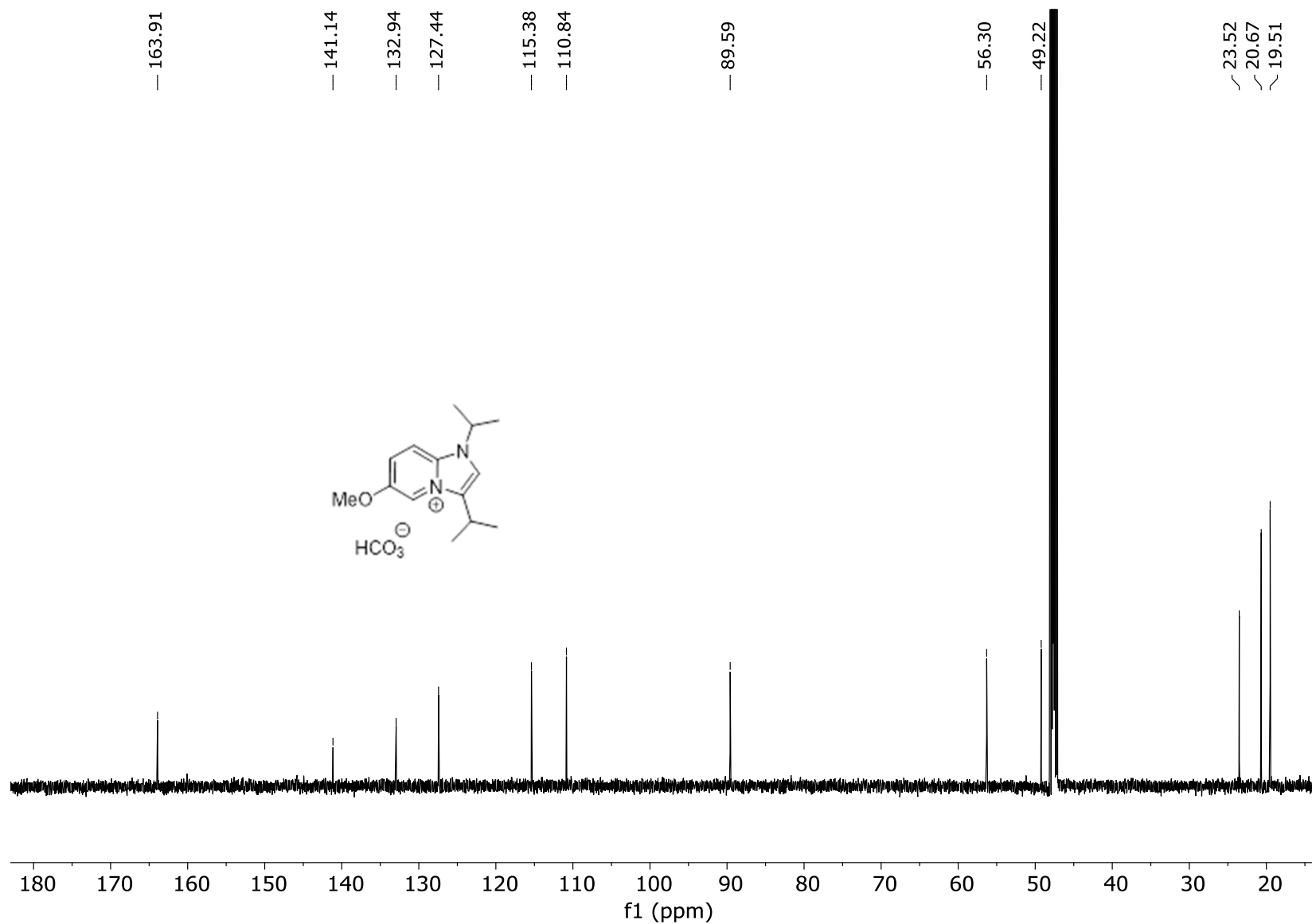
¹³C NMR spectrum of 1,3-diisopropyl-6-trifluoromethylimidazol[1,2-*a*] pyridine-4-ium hydrogen carbonate (**CF₃-NHC^{iPr}•H₂CO₃**), 126 MHz, CD₃OD



¹H NMR spectrum for 1,3-diisopropyl-6-methoxyimidazol[1,2-*a*] pyridine-4-ium hydrogen carbonate (500 MHz, CD₃OD)



^{13}C $\{^1\text{H}\}$ NMR spectrum for 1,3-diisopropyl-6-methoxyimidazol[1,2-*a*] pyridine-4-ium hydrogen carbonate (125 MHz, CD_3OD)



Electrochemical cell set-up

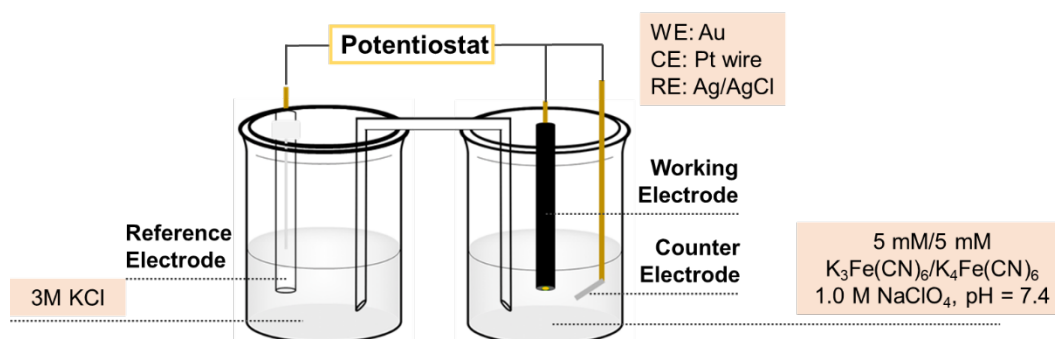


Figure S3: Electrochemical cell configuration

Electrode and SAM preparation

The organic contaminants on gold electrodes were removed by immersion in piranha solution ($H_2SO_4:H_2O_2 = 3:1$ v/v) for 30 seconds and washed with Milli-Q (MQ) water. Electrodes were manually polished in a figure-eight motion to smooth out the gold surface using 0.03 and 0.5 μ M alumina powder on a dampened spec-cloth. Alumina powder residue was removed from the gold electrodes by ultrasonication in MQ water, absolute ethanol and again with MQ water. Each ultrasonication was done for 10 mins. The electrodes were further electrochemically cleaned to remove any absorbed species during the polishing procedure. Pre-programmed cyclic voltammetry (CV) was used to clean the electrodes in base (0.5 M $NaOH_{(aq)}$) and acid (0.5 M $H_2SO_{4(aq)}$). For base cleaning, 100 CV cycles between 0 V and 2 V at a scan rate of 0.5 $V \cdot s^{-1}$. For acid cleaning, 100 CV cycles between 0 V and 1.5 V at a scan rate of 0.5 $V \cdot s^{-1}$. CV of the cleaned electrodes were immersed in 5 mM/5 mM $Fe(CN)_6^{3-/4-}$ and 1 M $NaClO_4$ in MQ water solution. The peak separation was approximately between 65–75 mV to ensure blank surface. The electrodes were rinsed with MQ water and dried under a stream of dry Ar before surface modification.

A freshly cleaned gold working electrode was modified by immersion of 10 mM solution of $MIC^{iPr} \cdot H_2CO_3$ in HPLC-grade MeOH for 24 h at 50 °C. The modified electrode was rinsed with MQ water and dried under a stream of Ar before electrochemical measurement.

Gold chips cleaning and SAM preparation

The gold chips were electrochemically cleaned in 0.5 M H_2SO_4 by running 100 CV cycles between 0 V and 1.6 V at a scan rate of 0.4 $V \cdot s^{-1}$. This procedure was repeated at least two times or until the cycles stabilized. The gold chips were rinsed with MQ water and dried under a stream of Ar before surface modification, using preparation similar to electrode functionalization.

Cyclic voltammetry stability of MIC^{iPr}

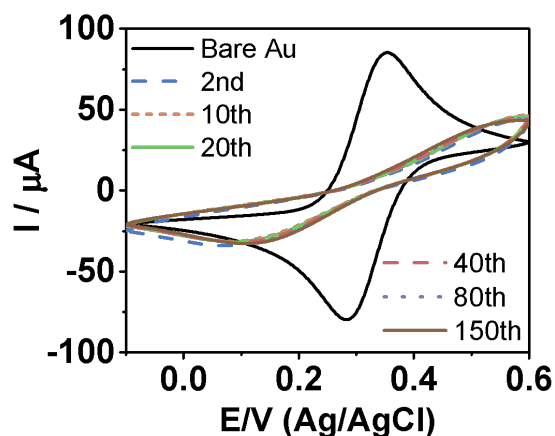


Figure S4: Cyclic voltammogram of **MIC^{iPr}** electrode indicating that the SAM is completely stable over repeated cycling up to 150 cycles between -0.1 and 0.6 V. The CV was obtained in a solution of 5 mM/5 mM $\text{Fe}(\text{CN})_6^{3-/4-}$ as the redox couple and 1 M NaClO_4 as the supporting electrolyte. The scan rate was set to 0.1 V s^{-1} . $\text{Ag}/\text{AgCl}/3 \text{ M}$ was used as the reference electrode.

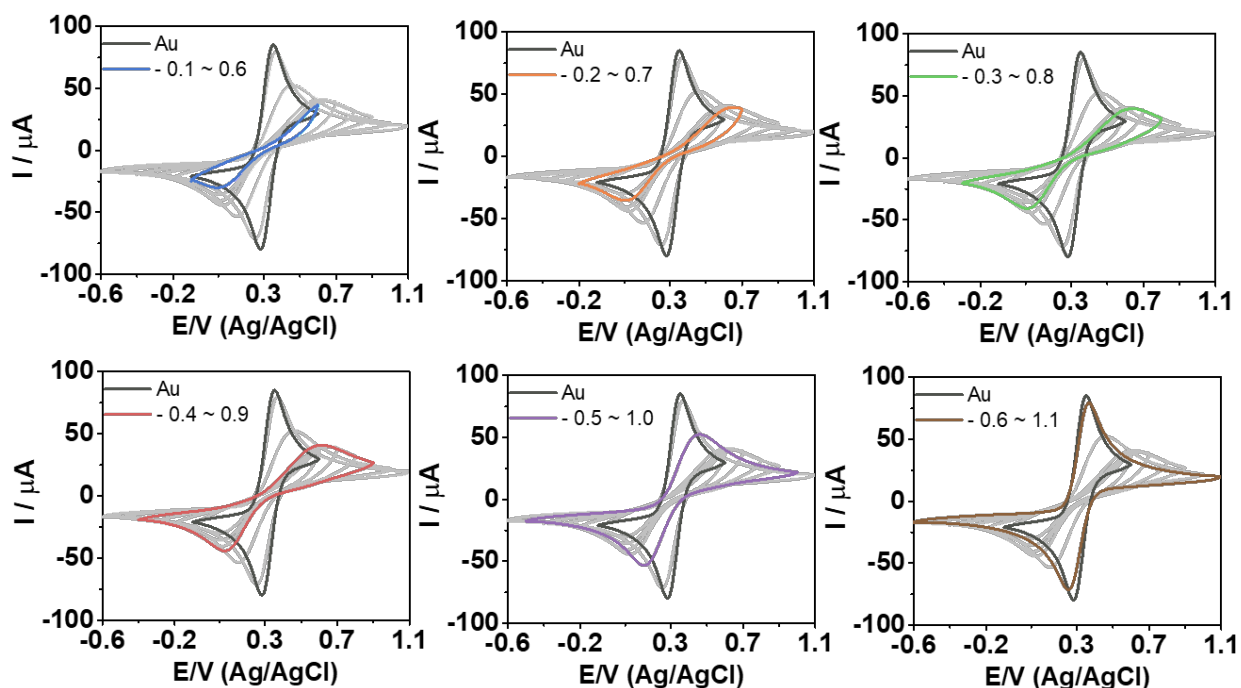


Figure S5: Cyclic voltammogram of **MIC^{iPr}** that shows repeated cycles for the reduction and oxidation of $\text{Fe}(\text{CN})_6^{3-}/\text{Fe}(\text{CN})_6^{4-}$ in solution with different potential windows. (a) -0.1 V to 0.6 V (b) -0.2 V to 0.7 V (c) -0.3 V to 0.8 V (d) -0.4 V to 0.9 V (e) -0.5 V to 1.0 V (f) -0.6 V to 1.1 V. The CV was obtained in a solution of 5 mM/5 mM $\text{Fe}(\text{CN})_6^{3-}/4-$ as the redox couple and 1 M NaClO_4 as the supporting electrolyte. The scan rate was set to 0.1 V s^{-1} . $\text{Ag}/\text{AgCl}/3 \text{ M}$ was used as the reference electrode

Electrochemical surface stripping with chronoamperometry

Electrochemical stability of **MIC^{iPr}** and **NHC^{iPr}** were tested using cathodic and anodic chronoamperometry stripping experiment. CV of **MIC^{iPr}** / **NHC^{iPr}** on gold electrode was measured in 5 mM/5 mM Fe(CN)₆^{3-/4-} as the redox couple and 1 M NaClO₄ as supporting electrolyte in MQ water solution. The electrode was then immersed 1 M NaClO₄ MQ water solution and chronoamperometry (CA) was performed for 30 seconds at a series of applied potential (from -0.5 to -1.2 V or 0.5 to 1.2 V). The electrode was then put back into the initial electrolyte solution and CV was measured. Some **MICs** still remained on surface even after -1.2 V exposure while **NHCs** were completely stripped away at -0.9 V (Figure 4). For anodic stripping experiment, both **MICs** and **NHCs** comes off at 1.2 V.

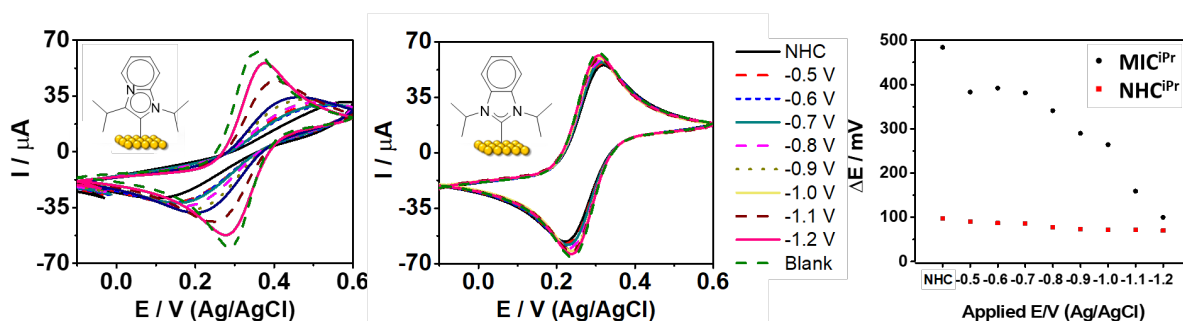


Figure S6: CV of **MIC^{iPr}** and **NHC^{iPr}** after each cathodic CA experiment stage from -0.5 to -1.2 V.

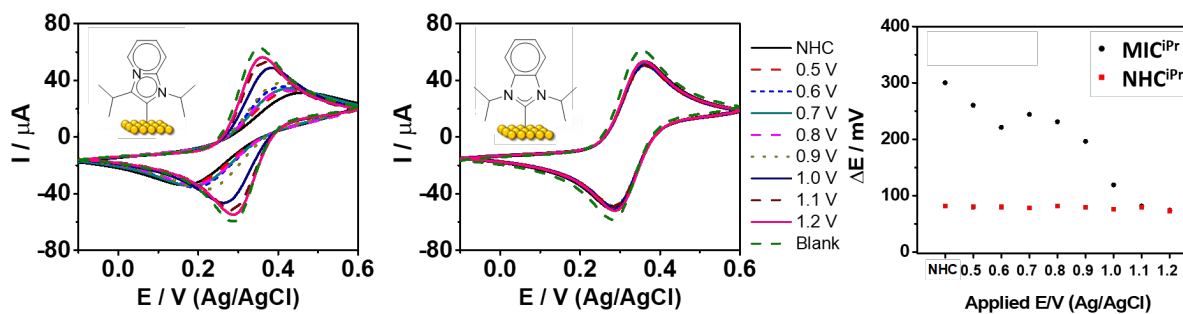


Figure S7: CV of **MIC^{iPr}** and **NHC^{iPr}** after each anodic CA experiment stage from 0.5 to 1.2 V.

X-ray photoelectron spectroscopy

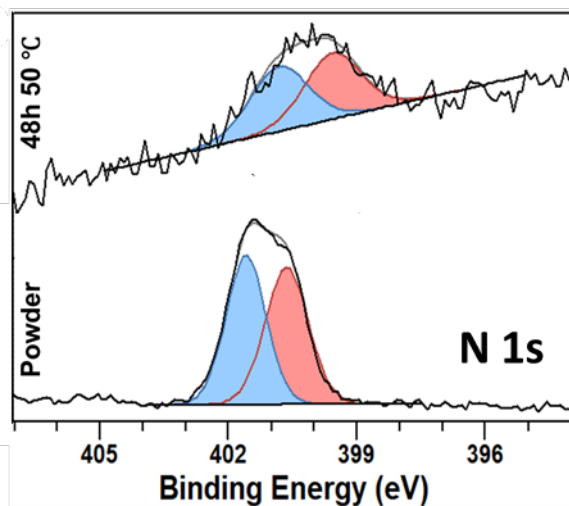


Figure S8: XPS N(1s) region comparing (top) a SAM prepared on a gold substrate under optimized conditions with (bottom) powdered samples of $\text{MIC}^{\text{ipr}} \cdot \text{H}_2\text{CO}_3$.

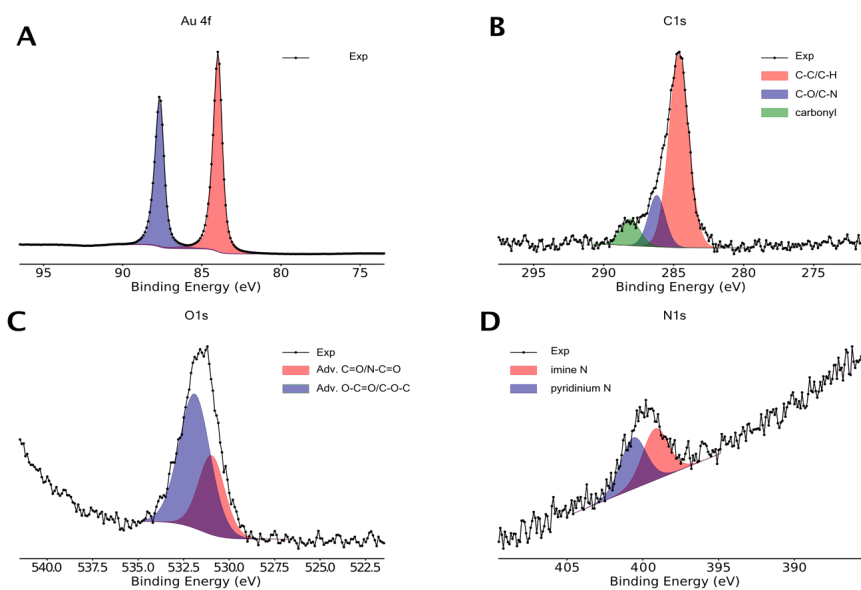


Figure S9: XPS analysis of MIC^{ipr} where deposition was 48 hours at 50 °C.

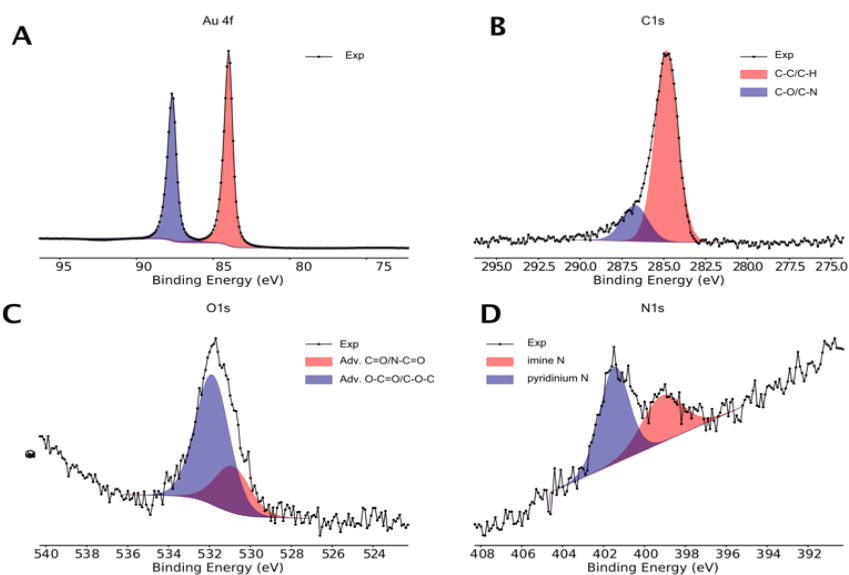


Figure S10: XPS analysis of MIC^{ipr} where deposition was 24 hours at room temperature.

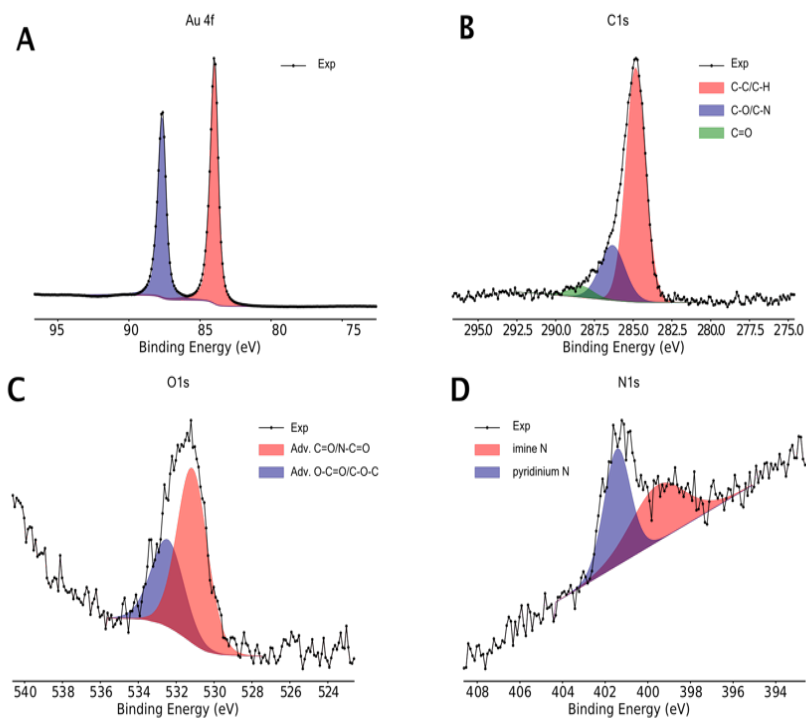


Figure S11: XPS analysis of MIC^{ipr} where deposition was 24 hours at 50 °C.

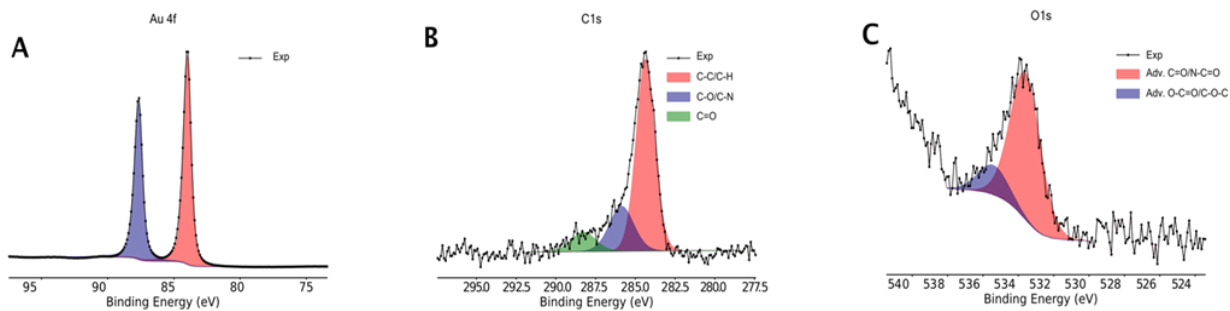


Figure S12: XPS analysis of MIC^{ipr} after 24 h in H_2O_2 .

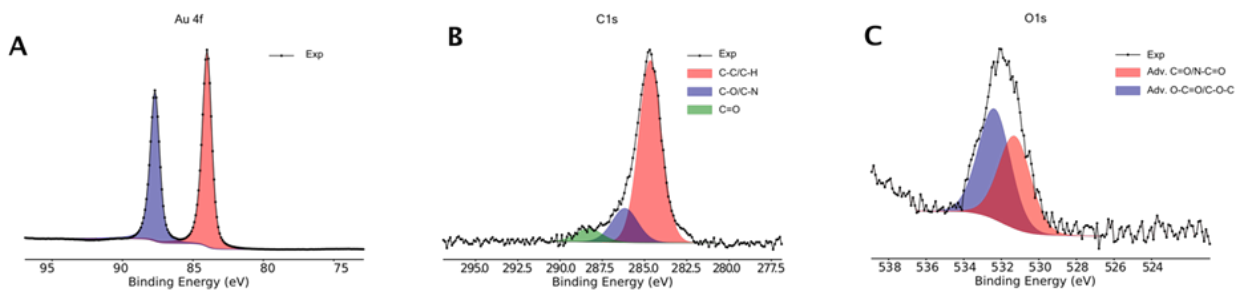


Figure S13: XPS analysis of MIC^{ipr} after 24 h in pH 2

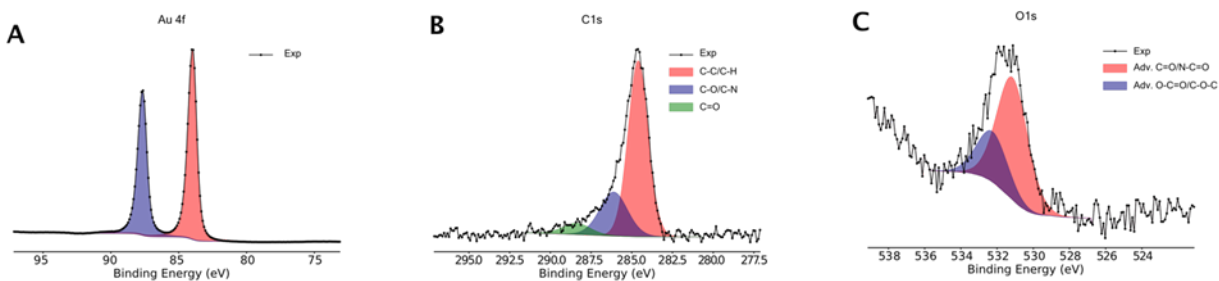


Figure S14: XPS analysis of MIC^{ipr} after 24 h in reflux water

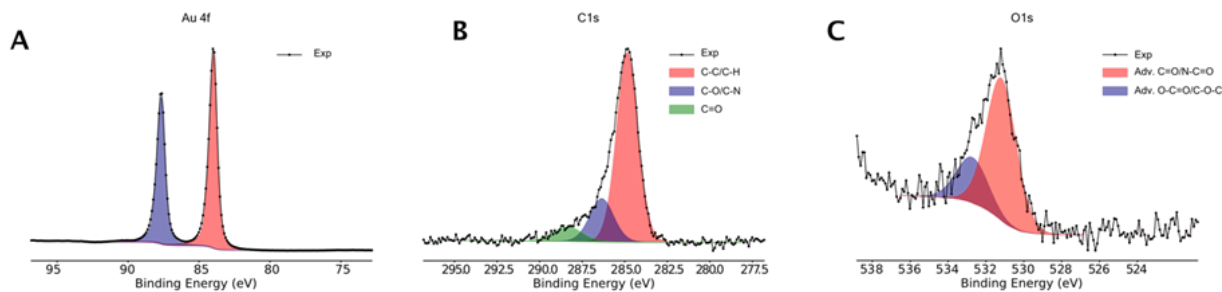


Figure S15: XPS analysis of MIC^{ipr} after 24 h in pH 12

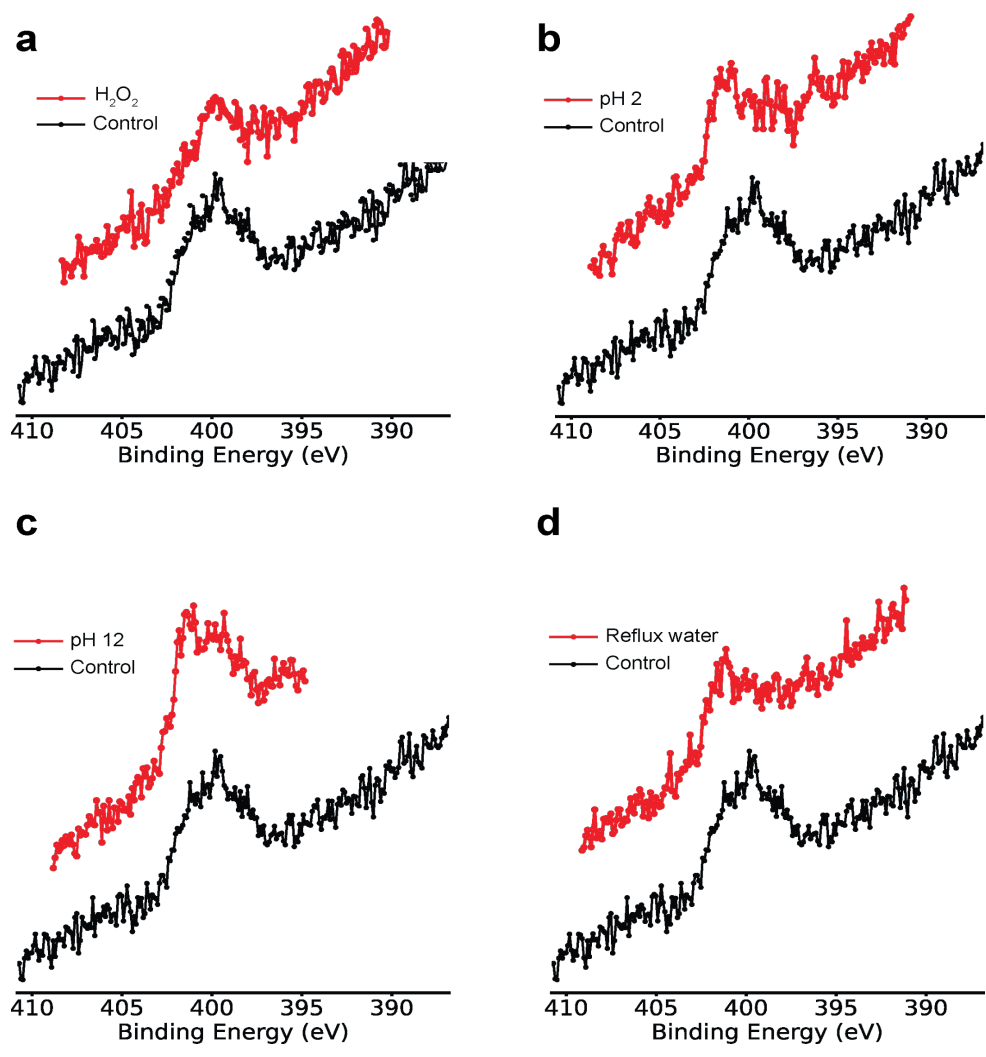


Figure S16: N 1s XPS analysis of MIC^{ipr} at different testing conditions compared to the control sample.

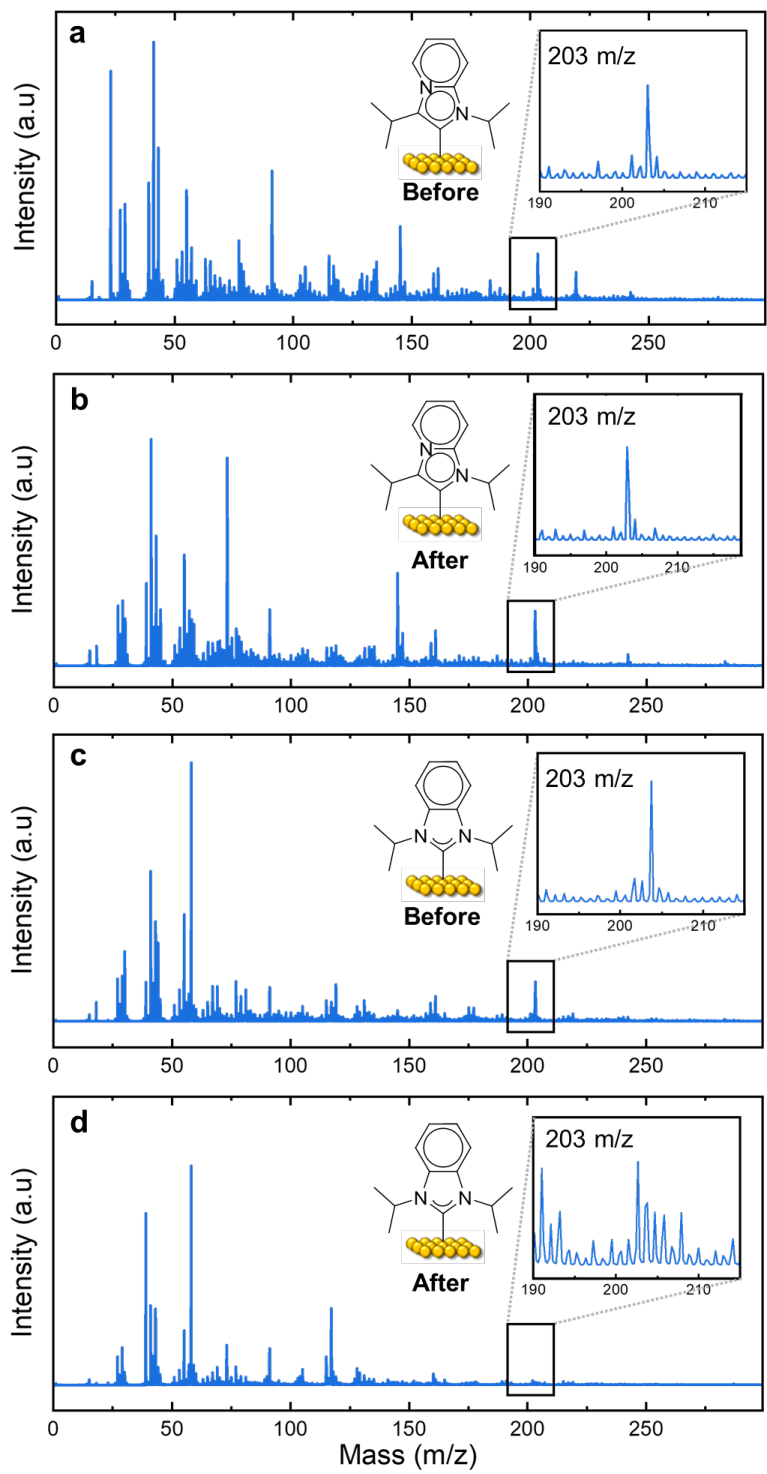


Figure S17: Full ToF-SIMS data of **MIC^{iPr}** and **NHC^{iPr}** before and after stability test under pH 12.

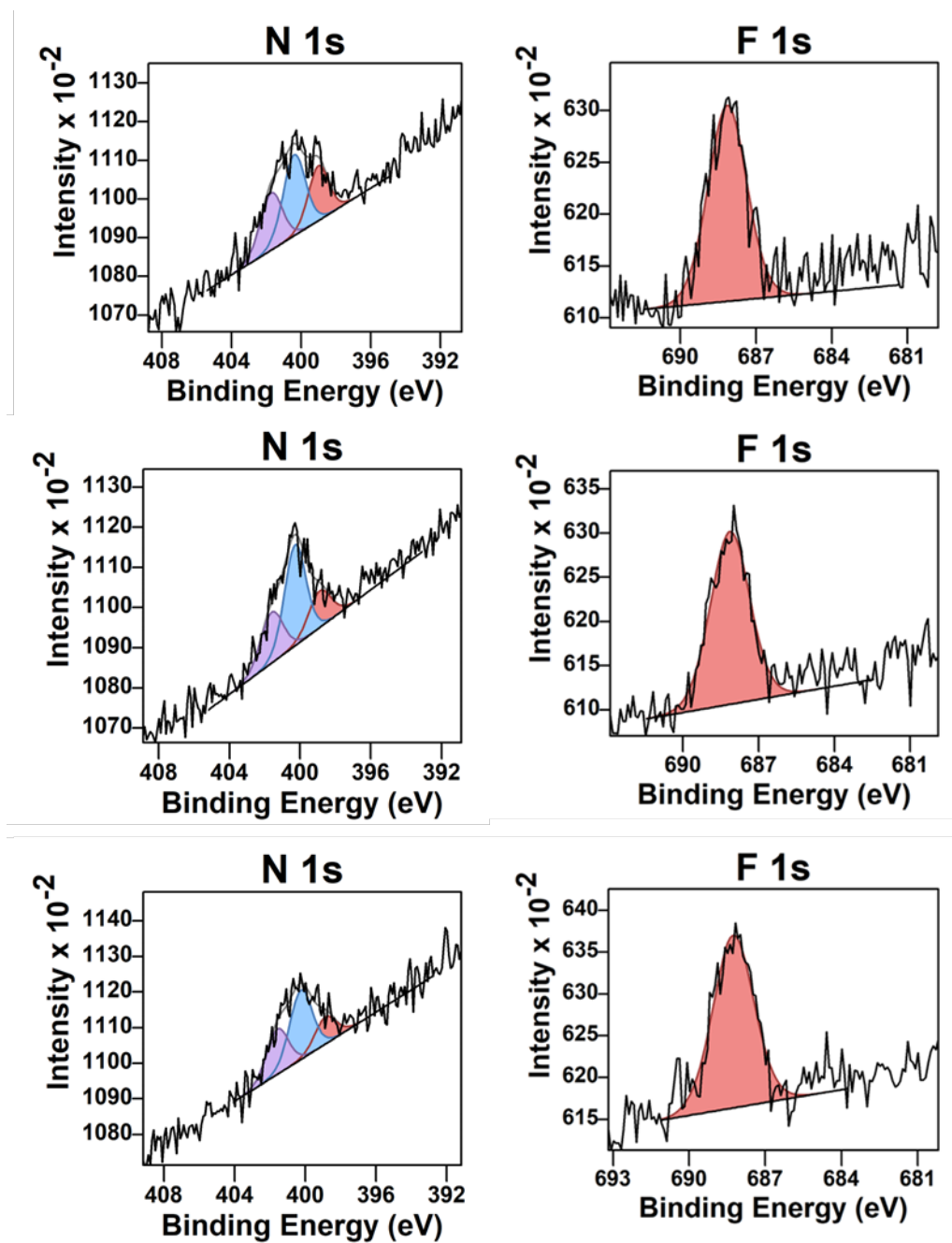
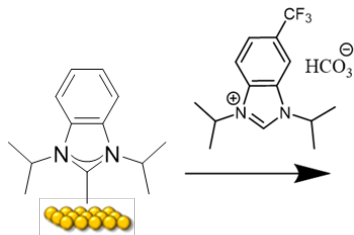
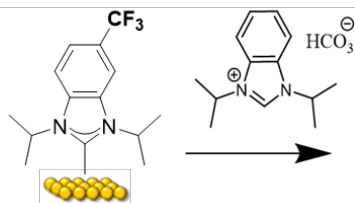
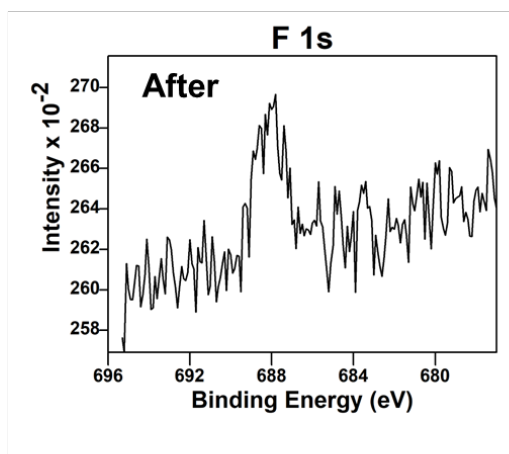
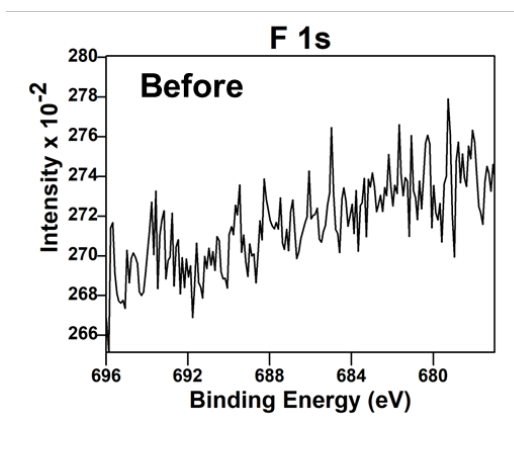


Figure S18: 3 sets of XPS data of co-deposition study with $\text{MIC}^{\text{iPr}} \cdot \text{H}_2\text{CO}_3$ and $\text{CF}_3\text{-NHC}^{\text{iPr}} \cdot \text{H}_2\text{CO}_3$. Purple and part of blue belongs to $\text{CF}_3\text{-NHC}^{\text{iPr}}$. Red and part of blue belongs to MIC^{iPr} .



F 1s Atomic Concentration %:

0 % → 1.53 %



F 1s Atomic Concentration %:

2.74 % → 1.40 %

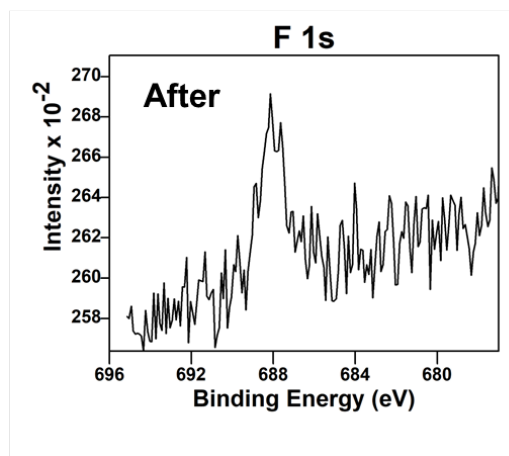
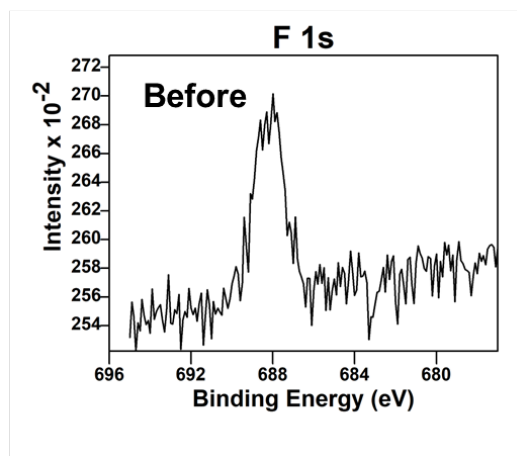
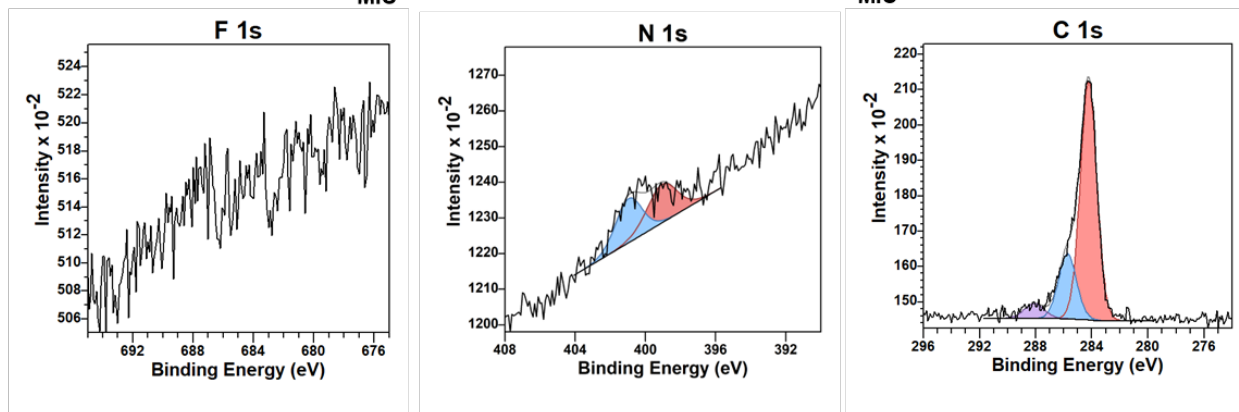
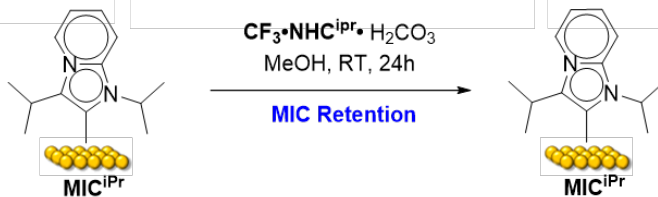
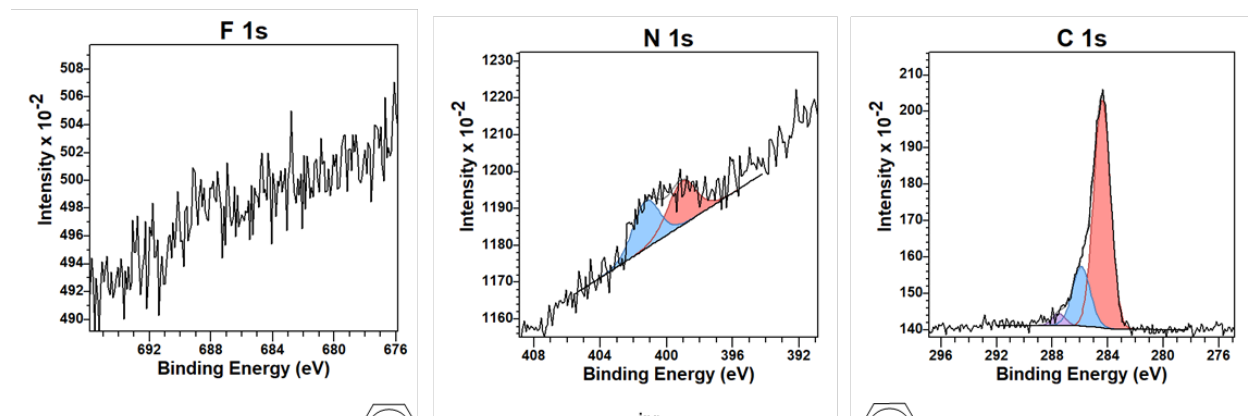
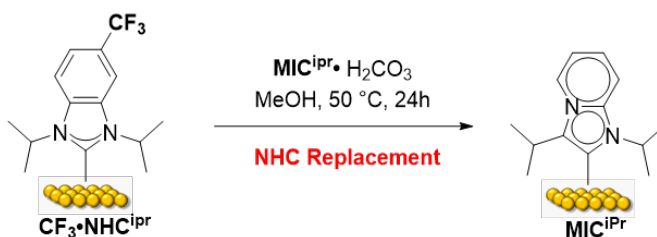


Figure S19: F 1s XPS spectra of replacement test between **NHC^{iPr}** and **CF₃-NHC^{iPr}**, and vice versa.

Replacement Test:



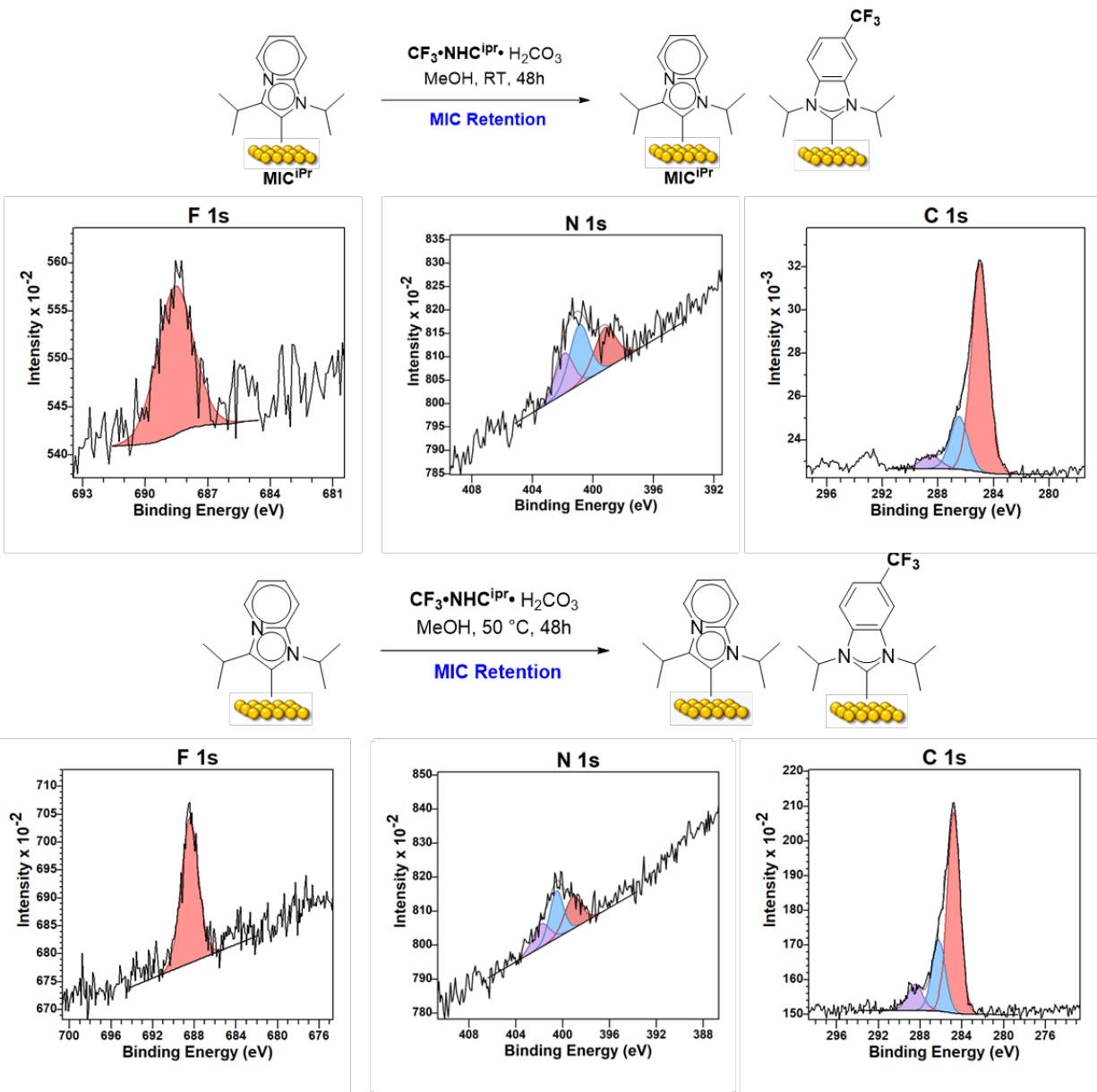


Figure S20: XPS analysis for replacement test between MIC^{iPr} and $\text{CF}_3\cdot\text{NHC}^{\text{iPr}}$.

Table S1: Area report of XPS analysis of co-deposition study.

Sample	Name	Position (eV)	Raw Area	Area / (RSF)	%At Conc	Ratio (N 1s of MIC ^{iPr} : F 1s)	Ratio (MIC ^{iPr} : CF ₃ -NHC ^{iPr})
1	F 1s	688.14	1233.33	233.6	0.81	1.5 : 0.81	5.55:1.00
	N 1s (red)	399.01	468.3	216.15	0.75		
	N 1s (blue)	400.4	756.43	349.24	1.21		
	N 1s (purple)	401.72	531.19	245.31	0.85		
2	F 1s	688.14	1296.72	245.6	0.86	1.06 : 0.86	3.70:1.00
	N 1s (red)	398.9	326.03	150.48	0.53		
	N 1s (blue)	400.29	855.76	395.07	1.38		
	N 1s (purple)	401.61	456.13	210.64	0.74		
3	F 1s	688.26	1417.33	268.43	0.92	0.82 : 0.92	2.67:1.00
	N 1s (red)	398.86	257.65	118.91	0.41		
	N 1s (blue)	400.25	703.53	324.78	1.12		
	N 1s (purple)	401.57	440.88	203.58	0.7		

Contact Angle:

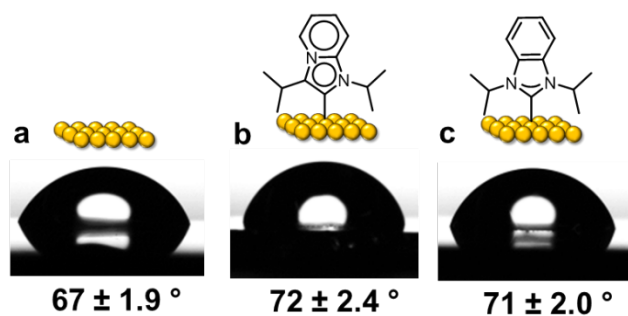

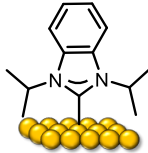
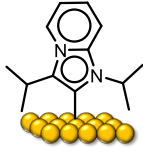


Figure S21: Contact angle for bare Au, NHC^{iPr}, and MIC^{iPr} SAMs.

Table S2: Contact angle measurements

Run #			
1	65.76°	71.51°	72.66°
2	68.71°	66.83°	69.23°
3	68.49°	71.35°	76.20°
4	63.93°	72.09°	70.75°

5	68.55°	71.99°	71.01°
---	--------	--------	--------

Contact angle analysis further provided evidence of the monolayer formation (Figure S21, Table S2). The surface hydrophobicity seemed to slightly increase after **MIC^{ipr}** deposition, although comparisons are within error. The contact angle of **MIC^{ipr}** was compared with **NHC^{ipr}** where no significant difference was observed. This similarity demonstrates that stronger C-Au bound **MIC^{ipr}** monolayer can be achieved without vastly changing the surface properties.

References

1. Crudden, C. M.; Horton, J. H.; Narouz, M. R.; Li, Z.; Smith, C. A.; Munro, K.; Baddeley, C. J.; Larrea, C. R.; Drevniok, B.; Thanabalasingam, B., Simple direct formation of self-assembled N-heterocyclic carbene monolayers on gold and their application in biosensing. *Nat. Commun.* **2016**, *7*, 12654.
2. Fulmer, G. R.; Miller, A. J.; Sherden, N. H.; Gottlieb, H. E.; Nudelman, A.; Stoltz, B. M.; Bercaw, J. E.; Goldberg, K. I., NMR chemical shifts of trace impurities: common laboratory solvents, organics, and gases in deuterated solvents relevant to the organometallic chemist. *Organometallics* **2010**, *29* (9), 2176-2179.
3. Beamson, G.; Briggs, D., *High Resolution XPS of Organic Polymers: The Scienta ESCA300 Database*. 1992.
4. Moulder, J. F.; Stickle, W. F.; Sobol, P. E.; Bomben, K. D., *Handbook of X-ray Photoelectron Spectroscopy*. Perkin-Elmer Corporation: 1992.
5. Arroniz, C.; Chaubet, G.; Anderson, E. A., Dual Oxidation State Tandem Catalysis in the Palladium-Catalyzed Isomerization of Alkynyl Epoxides to Furans. *ACS Catalysis* **2018**, *8* (9), 8290-8295.
6. Sheng, S.-R.; Huang, X., Polymer-supported 4-(phenylseleno)morpholine as a useful α -selenenylating agent for saturated aldehydes. A highly efficient route to α -haloaldehydes on solid phase. *Org. Prep. Proced. Int.* **2003**, *35* (4), 383-387.
7. Tan, J.; Ni, P.; Huang, H.; Deng, G.-J., Metal- and base-free synthesis of imidazo [1, 2-a] pyridines through elemental sulfur-initiated oxidative annulation of 2-aminopyridines and aldehydes. *Org. Biomol. Chem.* **2018**, *16* (23), 4227-4230.